Vaporization and decomposition of nitrogen trichloride in chlorine

NORAM Engineering / BC Research Inc.
2016

M. Gattrell, S. Berretta and C. Brereton

Abstract

The physical properties related to the vaporization of nitrogen trichloride (NCl_3) and chlorine mixtures are reviewed. The gas-phase decomposition of NCl_3 is also reviewed focusing on the influences of temperature and pressure. Experimental work is carried out investigating the gas-phase decomposition of NCl_3 in chlorine. Testing was carried out over the range of 20°C to 80°C, 1.4 to 3.4 bara total pressure and NCl_3 concentrations in chlorine from ~450 to ~4750 mg/kg.

The decomposition was found to be very temperature sensitive and autocatalytic. A reaction mechanism is presented that uses a mixture of available literature rate constants and values fitted to the measured experimental data. The work shows that NCl_3 in chlorine can be decomposed in the gas phase at close to ambient pressures with mild heating. This gas-phase NCl_3 decomposition could be coupled with a plug-flow vaporizer to safely vaporize and treat NCl_3 containing liquid chlorine. In addition, a concept for a safe atmospheric pressure chlorine vaporizer using a combination of gas stripping and gas phase NCl_3 thermal destruction is described.

Appears in: Pamphlet 21 "Nitrogen Trichloride - A Collection of Reports and Papers, Edition 8", Aug. 2023, The Chlorine Institute, Inc. https://www.chlorineinstitute.org/products/pamphlet-21-nitrogen-trichloride---a-collection-of-reports-and-papers-download-only

Table of Contents

1. Introduction

Nitrogen trichloride (NCl_3) is a highly unstable chemical that can decompose explosively. It can be inadvertently formed during the production of chlorine by the reaction of chlorine with trace ammonia or amine compounds in the feed chemicals. While only present at low concentrations in the product chlorine, it poses a significant danger if it accumulates at any point during processing or handling of liquid chlorine by the producer, transporter or end user. Because of this, the concentration of NCl_3 must be controlled to very low levels in liquid chlorine products. This means that chlorine producers need to be able to reliably and safely remove and destroy NCl_3 from their process. This report reviews NCl_3 properties related to the accumulation and safe destruction of NCl_3 and conducts some experimental investigations of the gas-phase NCl_3 destruction reactions.

2. NCl_3 properties

Nitrogen trichloride or trichloroamine (NCl_3) is a yellow, oily liquid (1.64 g/mL, m.p. <-40°C, b.p. 71°C (1,2)). It can be formed by the chlorination of ammonia (3):

$$NH_3 + 3\ Cl_2 \quad \Leftrightarrow \quad NCl_3 + 3\ HCl \qquad [1]$$

NCl_3 is sensitive to heat and shock and easily decomposes to its elements releasing significant energy (with the heat of formation of NCl_3 in CCl_4 being reported as 229 kJ/mole (4) and the free energy of formation in CCl_4 estimated at 301 kJ/mole (5)):

$$2\ NCl_3 \quad \Rightarrow \quad N_2 + 3\ Cl_2 + \text{heat} \qquad [2]$$

Because of the large amount of energy that can be released and its instability, the presence of any significant amount of NCl_3 can be hazardous. For a typical liquid chlorine pressure vessel (wall thickness 10-12 mm), the detonation of as little as 0.3 g/cm^2 wall area of liquid NCl_3 can overstress the metal and 1.5 g/cm^2 can fracture the vessel (1).

Aqueous solutions with NCl_3 contents exceeding solubility (>2000 ppm or about 17 mM NCl_3 (6)) are hazardous because a liquid NCl_3 phase can form. While for solvents with a higher NCl_3 solubility, such as carbon tetrachloride (CCl_4) or liquid chlorine, the maximum safe concentration typically depends on its subsequent processing. For the safe NCl_3 content in CCl_4 or liquid chlorine that is going to an NCl_3 thermal destruction unit, the maximum concentration is arrived at based on the potential temperature and pressure effects of the heat release from the NCl_3 decomposition (7). For product liquid chlorine, more stringent maximum concentrations are required because later evaporation of the liquid chlorine can leave a residue with a high concentration of NCl_3 (2).

3. NCl_3 vapor-liquid equilibrium

The accumulation of NCl_3 during liquid chlorine evaporation is driven by the relative volatility of liquid chlorine versus that of NCl_3 dissolved in the liquid chlorine. Unfortunately, because of the infrequent appearance of NCl_3 in the chemical industry and the danger of working with NCl_3, relatively little physical property data appears in the open literature.

The main source of experimental vapor pressure data is Apin's work from 1940 (8). However, these are only preliminary measurements taken while testing NCl_3's explosive properties rather than a detailed vapor pressure study. Unfortunately, to our knowledge no careful vapor pressure measurements have been reported in the literature. One must therefore rely on chemical structure-based methods to estimate properties. Using the method of Joback as described by Poling et al (9), one can estimate the various properties. The contributions to the physical properties from the different structural features are listed in Table 1.

Table 1: Parameters for Joback property estimations.

Structure (bonds)	**Property contribution**			
	tck (K)	pck (bar)	vck (cm^3/mole)	hvk (cal/mole)
N (3)	0.0169	0.0074	9	453
Cl (1)	0.0105	-0.0049	58	1083

These values can be used in a series of equations to estimate different properties, with the equation for estimating the heat of vaporization at the normal boiling point being:

$$\Delta H_{vap(bp)} = 15.30 + 0.004184 \sum_k N_k(hvk) = 15.30 + 0.004184\big(1(453) + 3(1083)\big) \quad [3]$$

In this manner the following estimated properties can be calculated:

T_c = 548 K, P_c = 56.4 bar, V_c = 201 cm^3/mole and $\Delta H_{vap(bp)}$ = 30.8 kJ/mole

A vapor pressure correlation is also available from the DIPPR databank (1), which gives:

$$Ln(p_{NCL3}) = A + B/T + C*LN(T) + D*T^E \quad [4]$$

With: A = 131.24, B = -8010, C = -16.91, D = 1.9677×10^{-5}, E = 2
P in Pa and T in K, and with ΔH_{vap} = 31.07 kJ/mole

One can see that the DIPPR ΔH_{vap} is similar to that estimated using the Joback approach from the open literature. The experimental data, the estimated vapor pressure from Yaws (10) (similar to DIPPR) and vapor pressure data for some structurally similar compounds are shown in Figure 1. One can see that the experimental data gives a lower dH_{vap} of about 23.9 kJ/mole and is not consistent with the other data.

4. NCl_3 activity in liquid chlorine

To determine the accumulation of NCl_3 while vaporizing liquid chlorine, the relative amounts of NCl_3 and Cl_2 being vaporized need to be estimated. A study by Zeller and DeJac has measured activity coefficients (γ) for low concentrations of NCl_3 in liquid chlorine at ~25°C (11). They fit their data with a two-suffix Margules model with A ≈ 1535 cal/mole (6.42 kJ/mole) at 25°C and x being a mole fraction.

$$\mathrm{RTln}(\gamma_{NCl3}) = A{x_{Cl2}}^2 \quad [5]$$

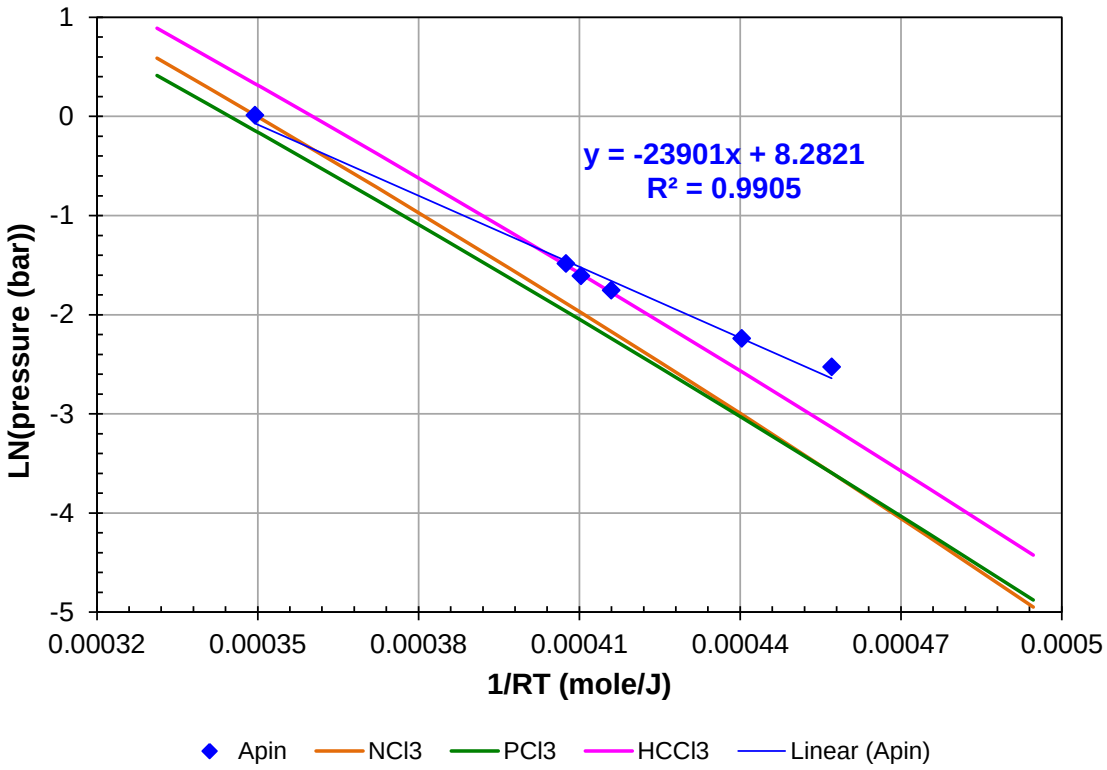

Figure 1: Some vapor pressure curves from Yaws (10) for NCl_3 and some structurally similar compounds along with the data from Apin (8) for NCl_3.

However, one can also use the method of Hildebrand and Scatchard (9) which also has a single adjustable interaction parameter (l_{12}) and so can be fit to Zeller and DeJac's limited set of data, but also makes use of the component properties (molar volumes and heats of vaporisation) to try to provide an improved estimation.

$$\mathrm{RTln}(\gamma_{NCl3}) = V_{NCl3}\varphi_{Cl2}^2[(\delta_{NCl3} - \delta_{Cl2})^2 + 2l_{12}\delta_{NCl3}\delta_{Cl2}] \quad [6]$$

Where:
V_i = the pure liquid molar volume
φ_i = the volume fraction of i

$$\varphi_{NCl3} = \frac{x_{NCl3}V_{NCl3}}{x_{NCl3}V_{NCl3} + x_{Cl2}V_{Cl2}}$$

δ_i = the solubility parameter

$$\delta_{NCl3} = \sqrt{\frac{\Delta U_{NCl3}}{V_{NCl3}}} = \sqrt{\frac{\Delta H_{Vap-NCl3} - RT}{V_{NCl3}}}$$

With all terms estimated at the same temperature, typically 25°C.

This approach, unlike the two-suffix Margules model, does not assume that the activity coefficients are symmetric and instead uses the different liquid molar volumes and heats of vaporization to estimate the different cohesive energy densities. This provides a better fit when the two components are of different sizes, though similar to the two-suffix Margules model it does

not extend well to polar mixtures. A comparison of the two approaches is shown in Figure 2, with the two models set to give the same infinite dilution activity coefficient (13.4) for NCl_3 in liquid chlorine. The models begin to differ as the concentration of NCl_3 increases with the Hildebrand and Scatchard model being about 1% lower at x_{NCl3} ~ 0.0045 (~7600 mg/kg).

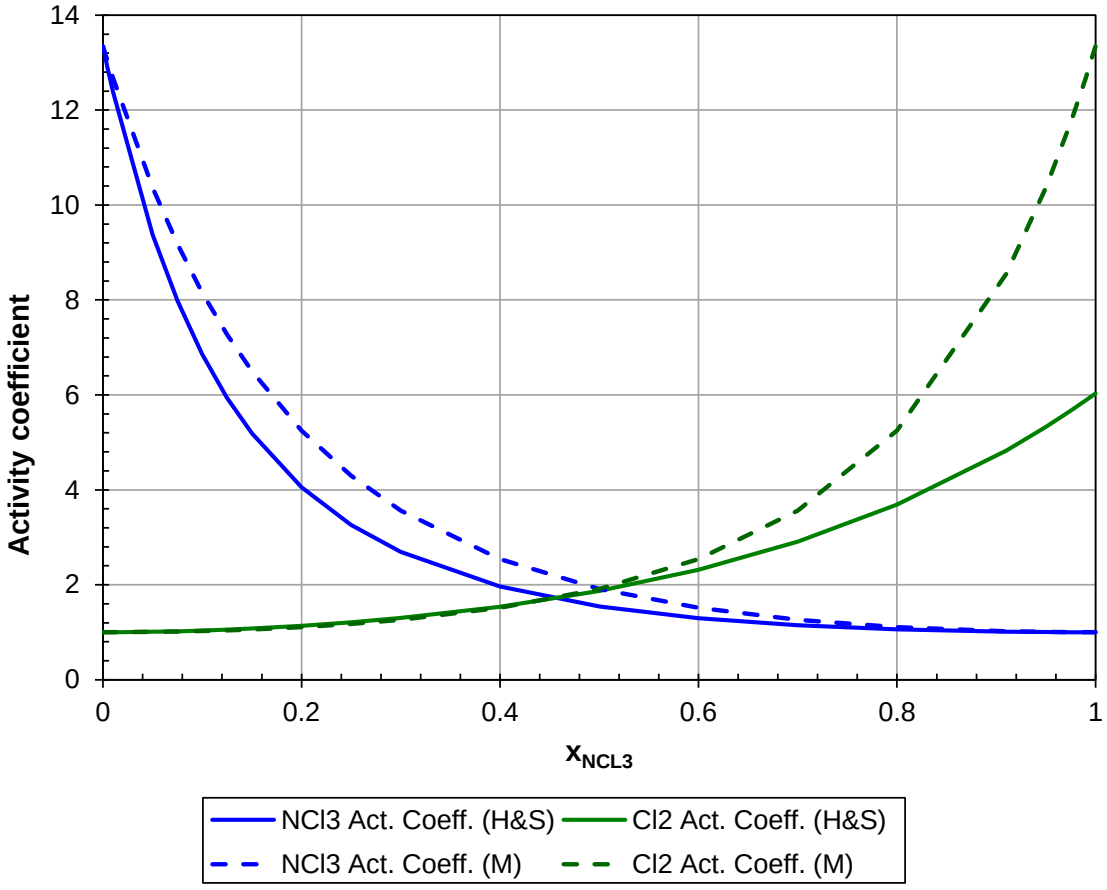

Figure 2: Estimated activity coefficients for NCl_3 and Cl_2 liquid mixtures at 25 C using the two-suffix Margules model (with A = 6.42 kJ/mole) and the Scatchard and Hildebrand model (with l_{12} = 0.1176) (NCl_3 in Cl_2 infinite dilution activity coefficient of 13.4).

In the work of Zeller and DeJac (11), 12 measurements were made of NCl_3 concentrations in liquid chlorine and in the gas phase above it at around 24.5°C and 98 psig. However, the liquid phase NCl_3 concentrations were from 1.1 to 12.9 mg/kg (x_{NCl3} from 6.5×10^{-7} to 7.6×10^{-6}) and the gas concentrations were from 0.1 to 2.6 mg/kg, making measurement errors a significant factor. This gave an average measured activity coefficient of 13.4, but with a standard deviation of 9.9.

Other data is available from a Solvay investigation where chlorine was evaporated from a flask containing NCl_3 in liquid chlorine (12). The starting and final liquid compositions were measured as well as the gas composition, allowing for a check on the mass balance. Higher NCl_3 concentrations were also used (1330 mg/kg increasing to 4830 mg/kg), which should result in lower measurement errors. The activity coefficient model in equation 6 can be used to integrate the NCl_3 vaporization, and it was found that a value of l_{12} = 0.092 gave the best fit. This corresponded to an infinite dilution activity coefficient of 12.5 for NCl_3 in liquid chlorine at the test conditions of -33°C or 7.7 at 25°C (assuming that RT Ln(γ) ≈ constant).

Similar data is available from FMC (13). They report the vaporization of 1850 lb of chlorine from an initial 2000 lb cylinder, which resulted in the NCl_3 concentration in the liquid increasing from 1 mg/kg to 11 mg/kg. Again, the activity coefficient model can be used to integrate the NCl_3 vaporization, and it was found in this case that a value of l_{12} = 0.096 gave the best fit. This corresponded to an infinite dilution activity coefficient of 14.0 at the test conditions of -33°C or 8.4 at 25°C.

These various data values are plotted in Figure 3. Overall, considering the high levels of error expected in measuring the very small concentrations involved, the results are reasonably consistent. The two highest and lowest 25°C infinite dilution activity coefficients from Zeller and DeJac were discarded, and the remaining 8 points were averaged along with the Solvay and FMC data. This gave an average 25°C infinite dilution activity coefficient of ~11.8, which would correspond to l_{12} = 0.112 for the Hildebrand and Scatchard model (the fitted curve in Figure 3). This is a relatively large value for the binary parameter (l_{12}), which may be due to the polarity of NCl_3 (9).

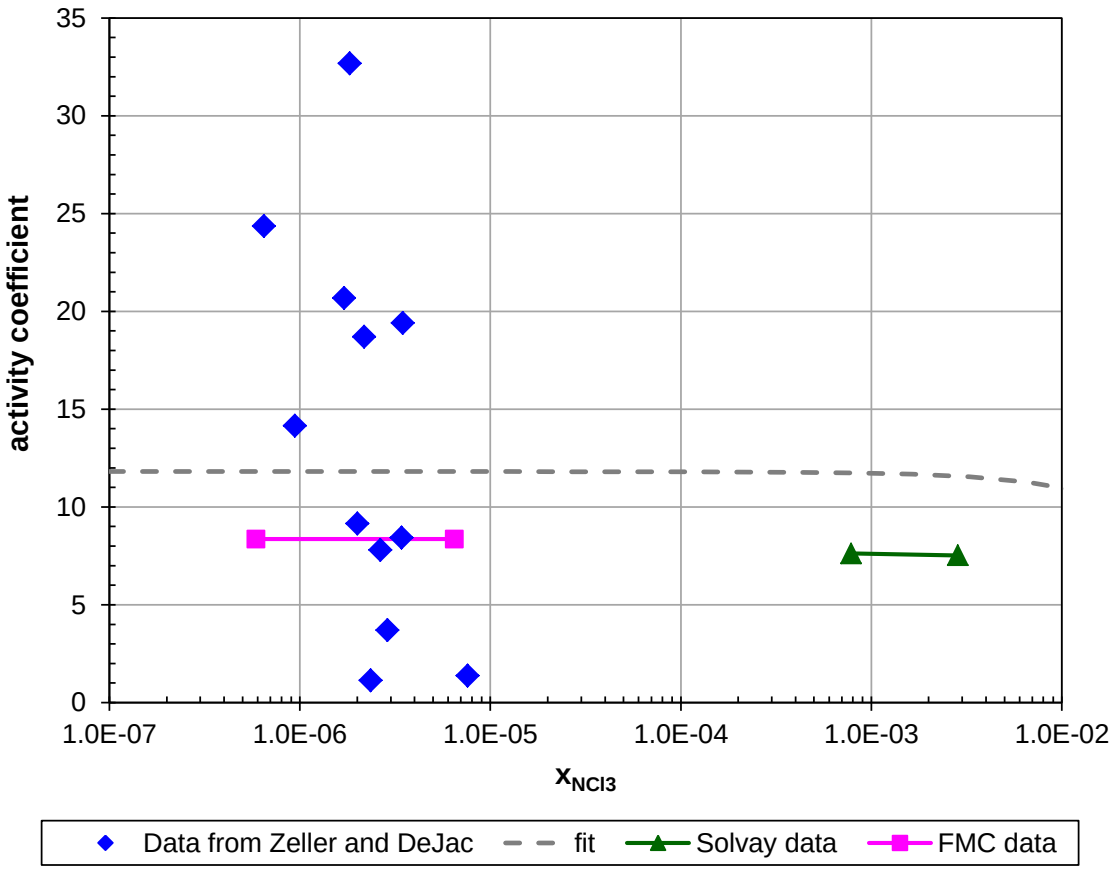

Figure 3: Activity coefficients estimated from different data sources. Solvay (12) and FMC (13) data has been converted to a 25°C basis.

Using vapor pressure estimates for pure NCl_3 and chlorine along with the estimated activity coefficients for the two compounds in a liquid mixture, one can calculate the expected concentration of a steady state liquid pool in a vaporizer (assuming no NCl_3 decomposition). The resulting plot for the case with a vaporizer feed of liquid chlorine containing 100 mg/kg of NCl_3 is

plotted in Figure 4. One can see that for atmospheric pressure evaporation (at -34°C), the NCl_3 concentration in a vaporizer might be expected to reach level of almost nine times the feed concentration.

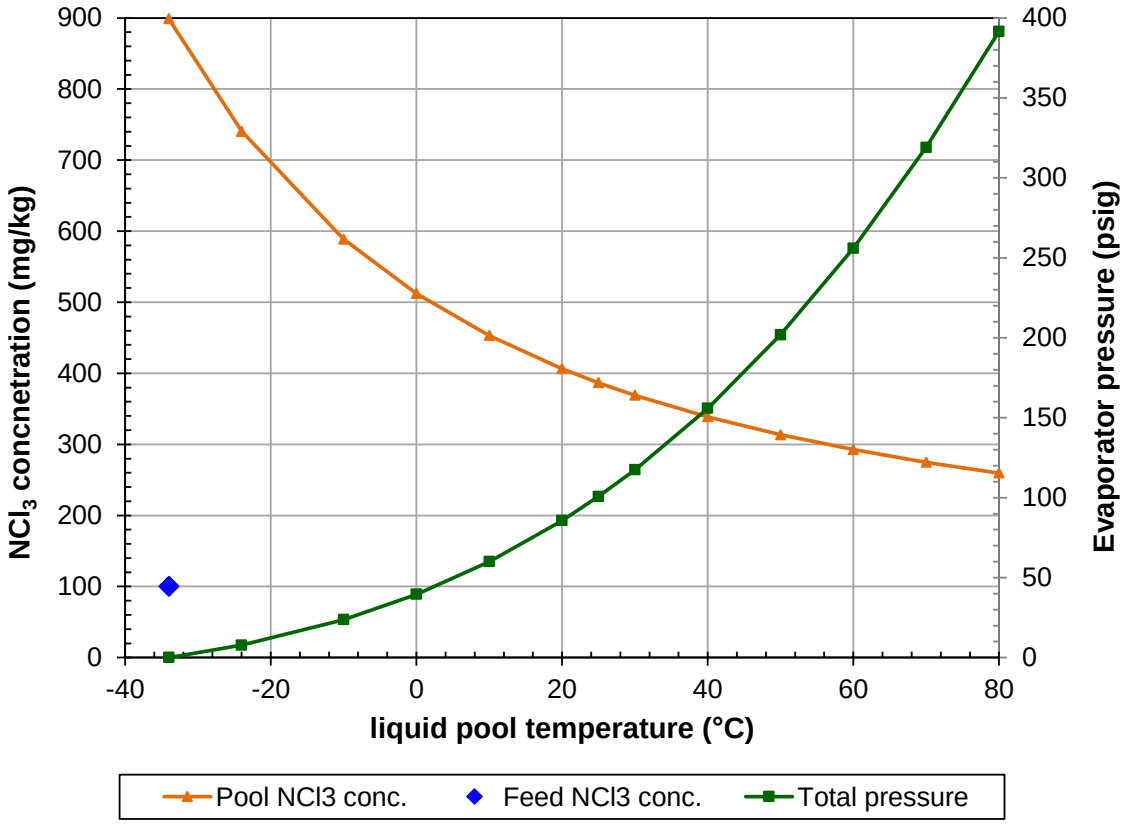

Figure 4: Calculated enhancement of NCl_3 concentration in a steady-state vaporizing pool of liquid chlorine at different temperatures with a feed containing 100 ppm. (NCl_3 and chlorine vapour pressures from Yaw's (10) and activities from the Scatchard and Hildebrand model with l_{12} = 0.112).

In considering the maximum safe concentration of NCl_3 in liquid chlorine in an area where it may become concentrated (e.g. a vaporizer, the residuals in the bottom of partially emptied liquid chlorine vessel, or at the bottom of a chlorine purification column) there are generally two considerations. One is the amount of temperature rise and pressure increase that might be expected if the NCl_3 in the liquid chlorine decomposed. A second concern is the possibility of the formation of a second phase of relatively pure, shock sensitive, highly explosive, liquid NCl_3. The possibility of a second phase in a two-component mixture is expected if (9):

$$\left(\frac{\partial^2 g^E}{\partial {x_1}^2}\right)_{T,P} + RT\left(\frac{1}{x_1} + \frac{1}{x_2}\right) < 0 \qquad [7]$$

Where:

$$g^E = RT\left(x_1 ln(\gamma_1) + x_2 ln(\gamma_2)\right)$$

These expressions can be evaluated using the activity coefficient models, to determine if phase splitting might occur. If phase splitting is indicated by the model, the composition of the phases can be estimated by numerically solving the models for:

$$(x_i\gamma_i)' = (x_i\gamma_i)" \qquad [8]$$

Where the apostrophes refer to the two phases. Using the further constraint that for each phase the mole fractions add to one then allows the equations to be solved.

It can be seen from Figure 5 that an NCl_3 rich phase appears possible at typical liquid chlorine operating temperatures. The worst-case prediction, using Zeller and DeJac's data fitted with the Margules model suggests an NCl_3 rich phase may appear at >8.5 wt% NCl_3 at -35°C or >19.6 wt% NCl_3 at 25°C. As can be seen for the two different Scatchard and Hildebrand model results, the results are sensitive to the infinite dilution activity coefficient used, with correct value being uncertain (as can be seen in Figure 3). For safety reasons, it is best to err on the conservative side.

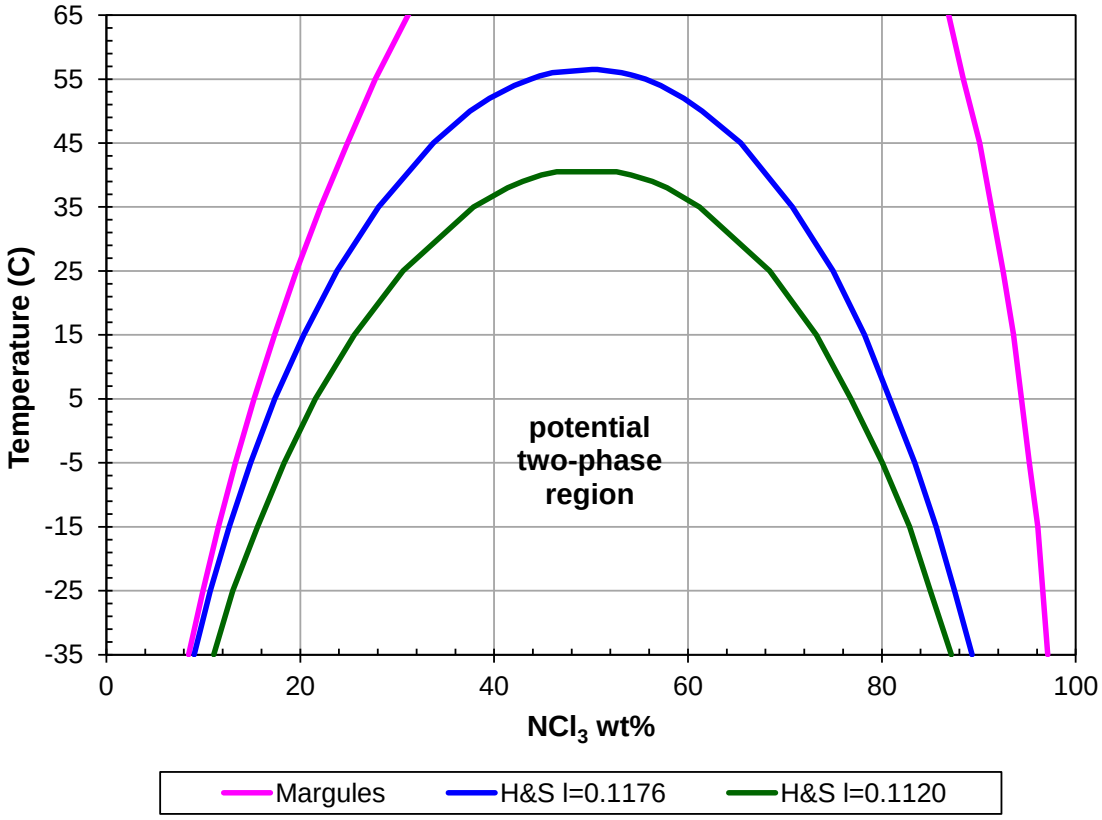

Figure 5: Estimated two-phase region for NCl_3 in liquid chlorine. Estimates made using Zeller and DeJac's data fitted with the Margules and the Scatchard and Hildebrand model (l_{12} = 0.118). Also, the estimate using the Scatchard and Hildebrand model fitted to the average 25°C infinite dilution activity coefficient from Figure 3 (l_{12} = 0.112).

Note that one should also consider the expected heat release from NCl_3 decomposition and calculate at what concentration this can no longer by absorbed by the vaporisation of the liquid chlorine. This calculation has been done by Piersma (7) who estimated that above ~13 wt% NCl_3, uncontrolled temperatures could occur, potentially leading to detonation. A similar calculation for NCl_3 dissolved in carbon tetrachloride estimated that the heat released by 8.6 wt% NCl_3 would be sufficient to completely vaporise the carbon tetrachloride. In an enclosed or

poorly vented vessel, one also has to consider the resulting pressure and so the NCl_3 concentration at which hazards may occur could be much lower. In guidelines for safe handling of liquid chlorine, reference is made to >3% NCl_3 in liquid chlorine giving rise to rapid, exothermic decomposition (1) and the decomposition of 6-8% NCl_3 in liquid chlorine giving rise to significant pressure depending on the headspace in the vessel (2).

To provide a safe margin, recommended limits in process equipment are <1 wt% from Euro Chlor (1) and <2 wt% from the Chlorine Institute (2). Depending on the frequency of analysis being used, an additional safety margin may need to be included.

5. NCl_3 in chlorine production

The various stages in chlorine production are diagrammed in Figure 6. Any ammonium or amine compounds present as impurities in the brine can be converted to NCl_3 by chlorine gas generated during the electrolysis step. The brine is typically acidified to ~pH 2 to maintain chlorine as volatile Cl_2, which is also in the best pH region for NCl_3 formation from ammonia, namely less than pH ~4 (1) and less than ~4 M HCl (14). Not all ammonia will be converted to NCl_3, with significant amounts likely lost due to side reactions that would generate nitrogen gas, chlorine and HCl (see, for example (15)). The exact losses will be plant and production rate dependent.

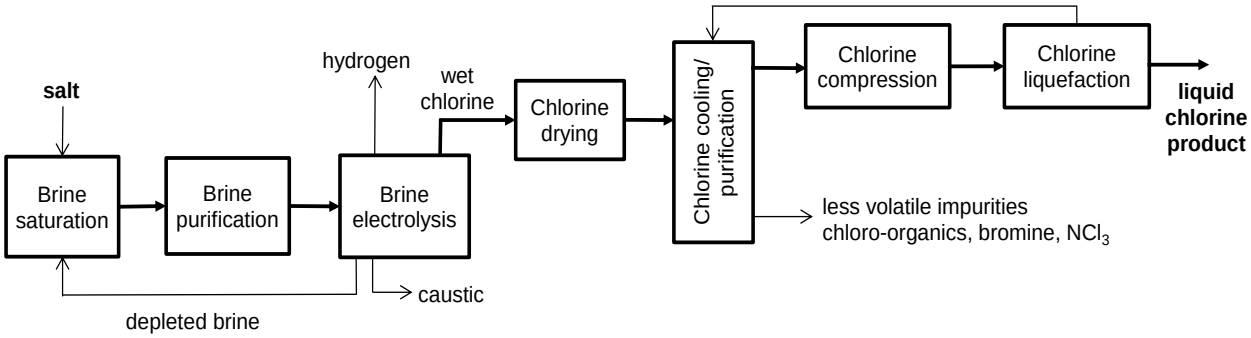

Figure 6: Stages in the production of liquid chlorine (17,18)

Because of its volatility, NCl_3 is carried from the brine electrolysis in the chlorine gas stream along with water vapour. The wet chlorine is then dried, with losses of NCl_3 during the drying step reported to be small (~12 %) (13,16).

Following the drying, the chlorine is often chilled and purified before compression. This is carried out using a counter-current column with liquid chlorine (≤ -34°C at atmospheric pressure) recycled from the liquefaction step (see Figure 7). While the rising chlorine gas is cooled and purified, the descending liquid chlorine collects less volatile impurities including NCl_3, bromine and chlorinated organics. This can result in a very low (<1 ppmw) residual NCl_3 in the final product liquid chlorine. However, because of the accumulation of NCl_3 in the liquid at the bottom of the column, care must be taken in choosing the approach for handling the column bottom liquid.

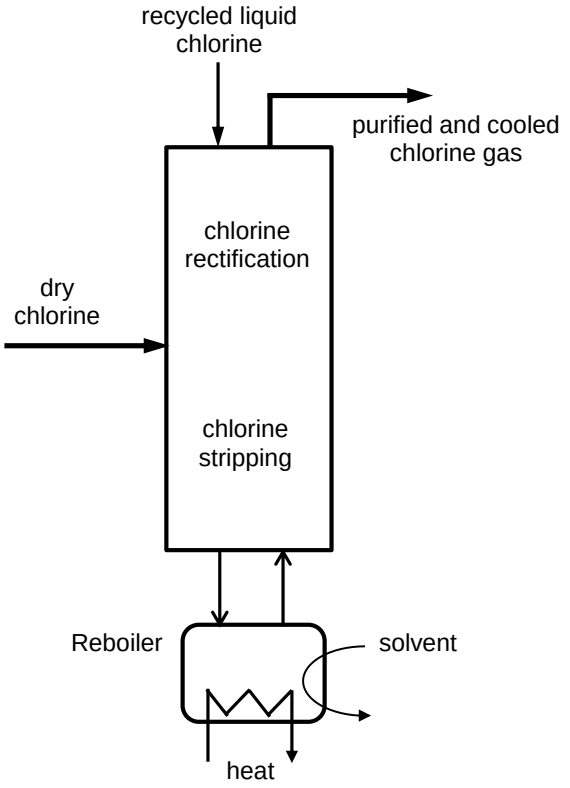

Figure 7: Chlorine chiller/scrubber/purification column.

6. NCl_3 treatment

Traditionally, the less volatile impurities were removed from the chlorine purifier bottom liquid by extracting using carbon tetrachloride. The carbon tetrachloride was then periodically transferred to a destruction reactor where it was gently heated (typically to 60-70°C (7)) with the decomposition reaction reported to be first order in NCl_3 with the rate constant given by (15,17,19):

$$k = 5.3x10^{19} exp\left(\frac{-E_a}{RT}\right) \quad [9]$$

With k in h^{-1}, temperature in K, and the activation energy (E_a) = 133.9 kJ/mole.

In refluxing carbon tetrachloride (b.p. 76.7°C), this gives a rate constant of 0.54 1/h, which for 90% destruction of the NCl_3 would require 4.3 h. The treated carbon tetrachloride could be returned to the chlorine purification column. Over time, the carbon tetrachloride would build up contaminants such as higher molecular weight chlorinated organics which required it to be sent for disposal and replaced with fresh solvent. With the discontinued use of carbon tetrachloride in the chemical industry (20), alternative methods for NCl_3 control have now been implemented.

One approach sometimes used to avoid NCl_3 is to remove ammonia compounds from the feed brine using chlorination under alkaline conditions (pH > 8.5) (17). This can be controlled to generate mono-chloramine which can be stripped from the brine and/or ammonia compounds can be decomposed to nitrogen gas using break point chlorination reactions (2,21,22). While this

method should avoid problems with NCl_3, the strong ability of the chlorine purification step to accumulate NCl_3 from any process upsets or unexpected sources of ammonia means that it is still a location for concern. Thus, the chlorine purifier column bottom liquid still requires careful monitoring and if the need arises, a method for treatment needs to be available.

The thermal destruction of NCl_3 can also be carried out in liquid chlorine, with reported very similar kinetics to those for carbon tetrachloride (1,17):

$$k = 7.46x10^{19} exp\left(\frac{-E_a}{RT}\right) \quad [10]$$

With k in h^{-1}, temperature in K and the activation energy (E_a) = 133.95 kJ/mole. However, to achieve similar rates to those for destruction in carbon tetrachloride would require similar temperatures. But for operation at, for example ~70°C, the vapour pressure of the liquid chlorine would be quite high at ~21 barg requiring expensive pressure-rated equipment. Also, it should be noted that in Differential Thermal Analysis (DTA) work the thermal decomposition of NCl_3 in liquid chlorine was found to show accelerating autocatalytic behaviour when tested in titanium or stainless steel test cells, but essentially a slow thermal decomposition when tested in a glass ampoule (18). Thus, suggesting the decomposition reaction in liquid chlorine is more complex than indicated by equation 10.

An alternative approach involves safely vaporising liquid chlorine by avoiding pool boiling that could otherwise concentrate the NCl_3 to hazardous levels. This can be accomplished using a plug-flow type vaporiser to produce an NCl_3 and chlorine gas stream (23). The resulting NCl_3 and chlorine gas stream can be used as a feedstock for production of hypochlorite, or it can be treated to decompose NCl_3 in the gas phase without the high pressures that would be encountered if thermally treating NCl_3 in liquid chlorine.

7. NCl_3 gas-phase decomposition

The gas phase decomposition reactions of NCl_3 are free radical reactions that can be initiated thermally (19), using an electric spark (24) or using chlorine atoms generated from chlorine gas by UV light (25) or a radio frequency discharge (26). The reaction is autocatalytic with a chain branching mechanism that can lead to detonation, though this detonation can be suppressed above critical total pressure that depends on temperature and the type of diluent gas (27). At higher pressures detonation can still occur at higher NCl_3 concentrations due to the additional contribution of thermal effects. NCl_3 concentrations of greater than ~3 mole% can support deflagrations and concentrations of greater than ~5 mole% can detonate (28). The decomposition reaction has been studied by a variety of groups resulting in a general outline of the possible mechanism and measurements of rate constants for some of the steps.

Key initial work looking at the gas phase decomposition mechanism of NCl_3 was carried out by Griffiths and Norrish (25,29,30). They used ultraviolet (UV) light to drive the decomposition of NCl_3 in chlorine and mixtures of chlorine and other gases. The reaction was followed by measuring the pressure increase while irradiating with light (the overall decomposition yields a volume increase (see equation 2)). During irradiation the pressure would typically linearly increase with time (a zero order reaction), then give a sharp increase near the completion. In “matured vessels” the reactions seemed to be primarily homogeneous in nature. The initiating step was considered to be the dissociation of chlorine gas (hence zero order in NCl_3):

$Cl_2 + hv \Rightarrow 2\ Cl^*$ [11]

With the atomic chlorine then rapidly reacting with the NCl_3 to generate the dichloramino radical:

$Cl^* + NCl_3 \Rightarrow Cl_2 + NCl_2^*$ [12]

They found that the quantum efficiency for NCl_3 destruction decreased with higher total gas pressure with different relationships for different gases. At lower pressures very high quantum efficiencies were found (as many as 20 NCl_3 reacted/hv), indicating a chain mechanism. The data could be fit by the relationship:

$$\varepsilon = \frac{1}{0.0038 p_{Cl2}} + \frac{1}{k_1 p_{gas}} + k_2 \quad [13]$$

Where:
ε = quantum efficiency (NCl_3 reacted per hv)
p_{gas} = the partial pressure of the gas in Torr

Where k_2 varied from 2.0 to 2.5 and the range studied was from p_{NCl3} 0.15 Torr to 2.48 Torr with the total pressures from 23 Torr to 708 Torr, resulting in 0.02-1.3 mole% NCl_3. For the testing with other gases, the chlorine/NCl_3 ratio was maintained at >85 to ensure that equation 11 remained the dominant initiating reaction and the values found for k_1 are listed in Table 2.

Table 2: Values of k_1 found experimentally (30)

Gas	k_1 (1/Torr)
Helium	0.00093
Argon	0.0016
Nitrogen	0.0017
Oxygen	0.0025
Carbon dioxide	0.0038

An investigation of the thermal decomposition of NCl_3 and the influence of total pressure was reported by Ashmore (27). The NCl_3 mixtures were prepared by mixing chlorine into a mixture of ammonia diluted by hydrogen or nitrogen at a pressure where the mixture was stable. The decompositions were then started by admitting the gas mixture into an evacuated, 3 cm internal diameter vessel to achieve a target, lower test pressure. Below certain critical pressures that depended on the gas mixture and the temperature, after an induction period the NCl_3 would explode (see Figure 8). As the pressure was increased closer to the critical upper pressure limit, the induction period was found to increase. This upper limit for explosive decomposition was insensitive to the concentration of NCl_3 once it was above 0.1% and remained so up to 2%, which was the highest concentration tested.

Above the critical upper pressure limit, the pressure-time curves followed an S-shape (see Figure 9), with the reaction rate rapidly slowing and the induction period becoming longer as the pressure is increased. Such an S-shaped curve is typical for an autocatalytic or chain branching reaction.

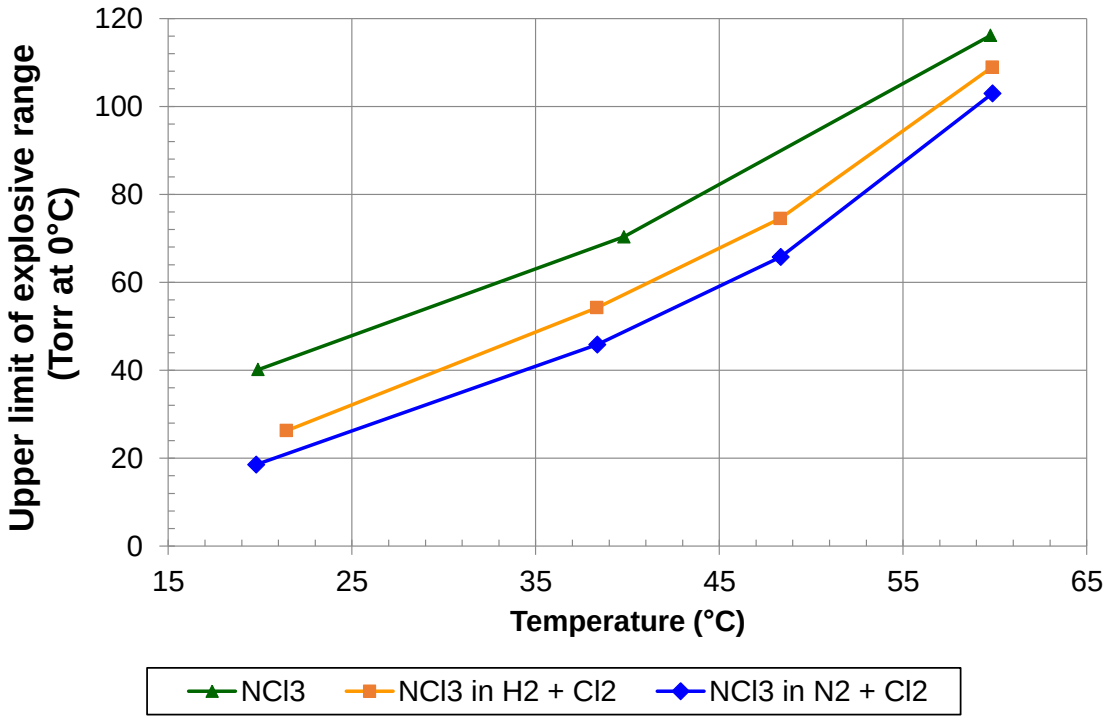

Figure 8: The influence of temperature on the upper explosion limit for different NCl_3 gas mixtures (27). Curves for pure NCl_3, 1% NCl_3 in equimolar H_2 and Cl_2, and 1% NCl_3 in equimolar N_2 and Cl_2.

For the thermally initiated decomposition of NCl_3, the initial reaction is thought to be the thermally initiated dissociation of NCl_3 (27):

$$NCl_3 \Leftrightarrow NCl_2^* + Cl^* \qquad [14]$$

The atomic chlorine generated would then rapidly react as shown in equation 12. The dichloramino radical was suggested to react according to a reaction such as:

$$NCl_2^* + NCl_3 \Rightarrow N_2 + m\ Cl^* + (5\text{-}m)/2\ Cl_2 \qquad [15]$$

Where, m varies from 1 to 5. For m = 1, each dichloramino radical generates one atomic chlorine which can regenerate the dichloramino radical through equation 12. For m > 1, there would be a net production of radicals and so an accelerating effect on the overall NCl_3 decomposition reaction.

These later steps in the gas phase decomposition mechanism were studied in more detail by Clark and Clyne (26,31,32). In their work, they used microwave or radio frequency discharges to generate atomic chlorine from chlorine gas. The atomic chlorine was mixed with NCl_3 gas and the reactions were followed using UV absorption, which allowed the measurement of NCl_3 and NCl_2^*. They also found that a coil of nickel wire could be used to remove Cl*, but with no detectable heterogeneous reaction of NCl_2^*. This allowed them to generate samples of dichloramino radical. Using this approach, they were able to measure the concentrations of different species with time and so to determine reaction orders and rate constants.

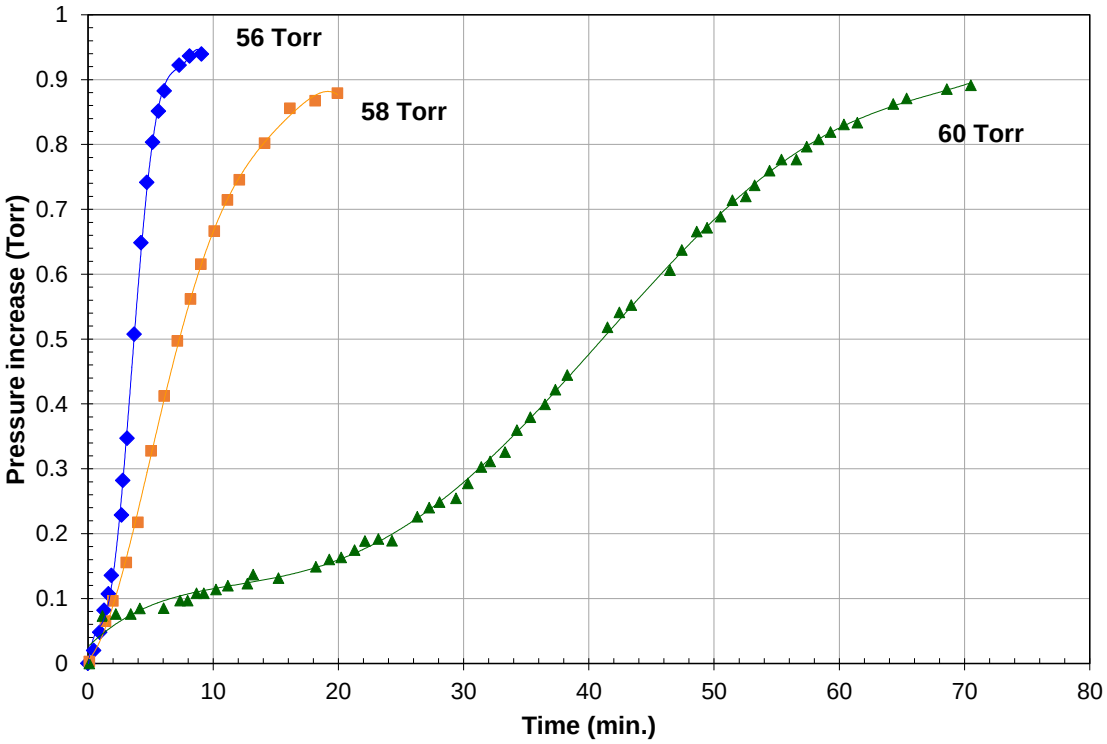

Figure 9: Pressure-time curves for the decomposition of NCl_3 in an equimolar mixture of H_2 and Cl_2 at 38.4°C (27). The decomposition rate can be seen to dramatically slow as the pressures are increased above the upper limit for explosion, which was ~55 Torr for the given conditions.

The rate for equation 12 was estimated as $k_{12} = 7.9 \times 10^{11}$ $cm^3mole^{-1}s^{-1}$ at 25°C (32) based on competition with the reaction of chlorine atoms with added nitrosyl ($k = 2.0 \times 10^{11}$ $cm^3mole^{-1}s^{-1}$ at 25°C and with accounting for a 2.5 times concentration difference used in the test). However, the recommended value for the rate of the reaction of chlorine atoms with nitrosyl has since been revised upwards ($k = 4.9 \times 10^{13}$ $cm^3mole^{-1}s^{-1}$ (33)) and so an updated estimated rate would be $k_{12} = 2.0 \times 10^{12}$ $cm^3mole^{-1}s^{-1}$ at 25°C.

Under the reaction conditions used, the main following reaction of the dichloramino radical was:

$$2\ NCl_2^* \Rightarrow N_2 + n\ Cl^* + (4-n)/2\ Cl_2 \qquad [16]$$

The rate was found to be pressure independent with $k_{16} = 5.01 \times 10^{11}$ $cm^3mole^{-1}s^{-1}$ and with $E_a \approx 0$. Over the range of conditions tested: -14 to 100°C and 0.8 to 3.1 mbara total pressure (around 0.01 mbara NCl_3, varying Cl* from much less than NCl_3 to 10-20 times greater, and with the balance Ar), the value for n was determined to be 1.8 ± 0.4. Under their reaction conditions, they found no sign of reaction 15.

An extensive series of papers from the Russian Academy of Sciences from 1975 to 2004 has examined the propagation of NCl_3 flames. They worked with mixtures of NCl_3 in helium and measured flame speeds across reactors as well as properties of stationary flames. Measurement techniques included: electron spin resonance (ESR) spectroscopy, temperature

measurements, pressure measurements, UV spectroscopy, chemiluminescence, and flame propagation rate.

The electron spin resonance (ESR) spectroscopy measurements on the stationary flame showed the presence of atomic chlorine (34). Testing flames using up to 20% NCl_3 in He, the concentration of atomic chlorine was found to reach 50% of the starting NCl_3 concentration for a range of 2-7 x 10^{-15} molecules/cm^3 NCl_3 (35). These results confirm, as shown in equation 12, that atomic chlorine is a key intermediate in the decomposition reaction. The maximum atomic chlorine signal occurred near the end of the visible part of the flame, with the visible chemiluminescence of the flame corresponding to excited chlorine molecules.

They also determined a lower as well as an upper pressure limit for an explosive range. Using a 70 cm long by 4 cm diameter glass reactor, with the surface treated with MgO, they found that for temperatures less than 70°C explosions (autoignition) did not occur at pressures less than 10 Torr (24). Working at 1 to 5 Torr and ~20°C (and so below the autoignition limit) an electric spark could be used to ignite the mixture and generate a flame which travelled along the reactor. The flames were essentially isothermal with heating measured to be less than 2°C for a 3% NCl_3 in He mixture. Stationary flames were also studied using a quartz reactor, surface treated with phosphoric acid. Using NCl_3 in He mixtures from 2 to 20% at pressures from 1 to 4 Torr and at 22°C a maximum flame heating of 3°C was found. This essentially isothermal flame propagation points to a chain reaction with reactive intermediates (chain carriers) propagating the flame.

It was also found that the maximum chemiluminescence, which is considered to be due to excited chlorine molecules, occurred around the point of maximum rate of decrease in NCl_3 concentration as opposed to the maximum concentration of chlorine atoms (36). This suggests that excited chlorine molecules (Cl_2') are being generated by reactions such as equations 15 or 16, rather than simply by the recombination of chlorine atoms. This is also consistent with the longer wavelength of the emission compared to that produced by the recombination of chlorine atoms (31).

The effect of diluent gases on the flame propagation was also investigated, with the reaction of NCl_3 in various other gases being initiated by heating at one end of the reactor at 1 degree/s until ignition occurred (19). An example of a series of results is shown in Figure 10. The authors suggest that at pressures below the pressure of peak flame velocity, increasing pressure results in slower diffusion of reactive intermediates to the reactor walls and so decreasing losses through quenching (heterogeneous chain breaking). At pressures above the pressure of peak flame velocity, higher total pressures result in damping of reactive intermediates by the diluent gases becoming more important (homogeneous chain breaking). It is interesting to note that the ignitable regions shown in Figure 10 increase with the NCl_3 concentration. As concentrations of NCl_3 further increase, the heat of reaction also begins to play a role in flame propagation, and it is reported that at 4% NCl_3 no upper limit for flame propagation is found (37). This is in general agreement with the results of Baillou, who found that NCl_3 concentrations of >~3 mole% can support deflagrations (28).

However, while there is a significant amount of work on the gas-phase decomposition of NCl_3, there is little experimental data at concentrations, temperatures and pressures of relevance to the chlorine industry. This work therefore aims to measure new decomposition rate data at close to ambient pressures, slightly elevated temperatures and NCl_3 concentrations in the 1000 ppmw range. In this way it hoped to extend the previously developed understanding of the NCl_3 decomposition reactions to more industrially relevant conditions.

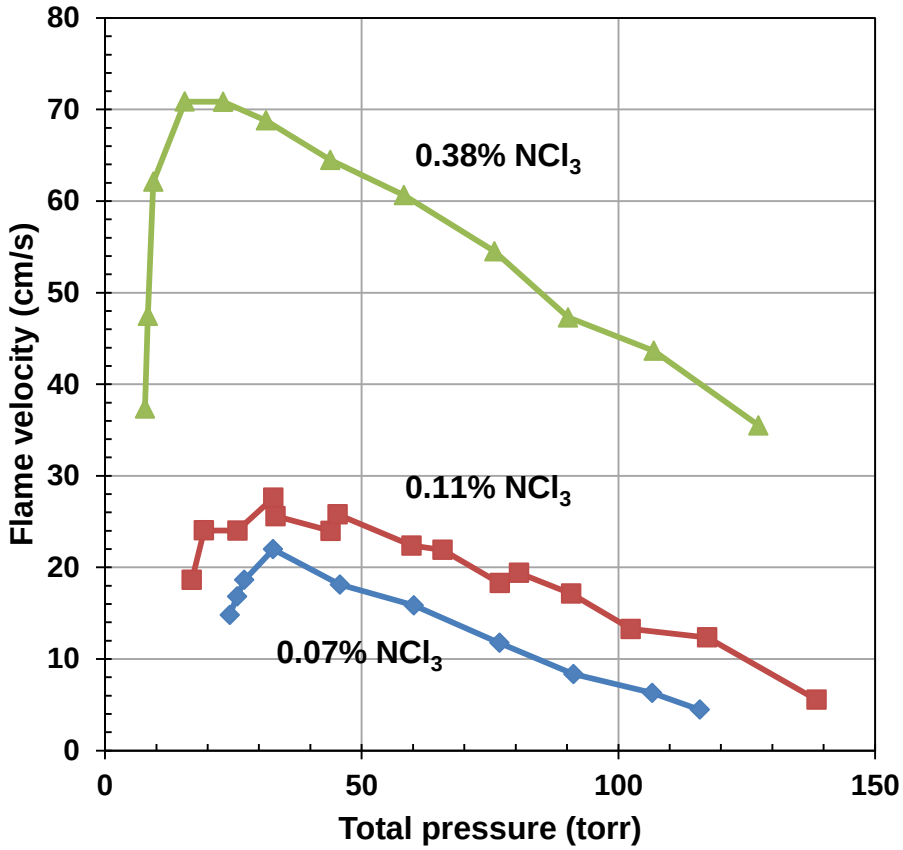

Figure 10: Influence of total system pressure on the velocity of the NCl_3 flame for different concentrations of NCl_3 in He at room temperature (38).

8. Experimental

8.1 Test equipment

A diagram of the test system is shown in Figure 11 and a photograph of the system assembled in a fume hood before heating tape and insulation have been added is shown in Figure 12.

The first part of the system (the NCl_3 synthesis reactor) reacts chlorine and ammonia to generate a stream of dry chlorine gas containing a target amount of NCl_3. This is heated by passing it through stainless steel tubing immersed in a hot oil bath to provide precise control of the maximum tubing wall temperature. The gas then enters a heat traced reactor (the NCl_3 decomposition reactor) where it is held for a period of time to allow NCl_3 decomposition reactions to occur. This is followed by a pressure gauge and backpressure regulator to allow control of the system pressure. Finally, the chlorine gas and any remaining NCl_3 are bubbled through a scrubbing tank containing a solution of sodium hydroxide and sodium sulphite to capture and treat the system exit gases. It was also possible to add additional gases to the main gas flow, with tests done using nitrogen, air and bromine.

A sampling system allowed a fraction of the gas flow to be diverted through a rotameter and then a gas bubbler. The gas bubbler contained concentrated HCl to absorb any NCl_3. Samples

could be drawn from: after the NCl_3 synthesis, after the gases had been heated but before entering the NCl_3 decomposition reactor, and after exiting the NCl_3 decomposition reactor. The first sampling location was used when troubleshooting the NCl_3 synthesis reactor, while for NCl_3 decomposition testing samples were taken before and after the decomposition reactor.

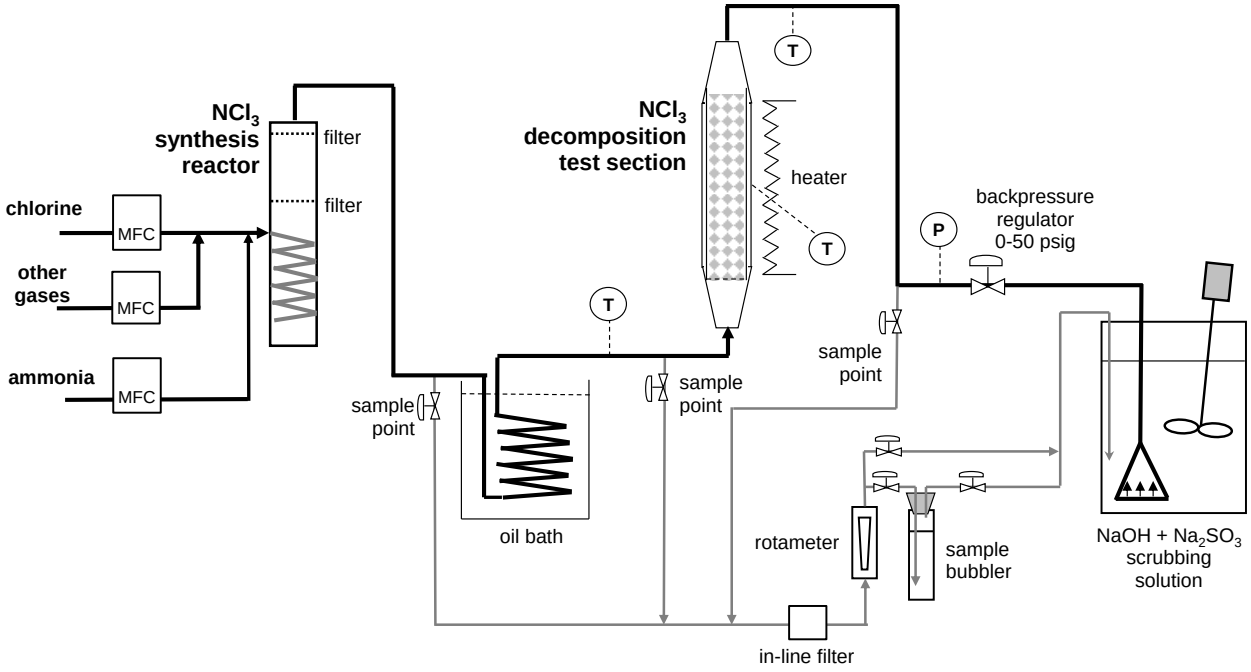

Figure 11: Diagram of the test system. Chlorine and ammonia gases are metered through mass flow controllers (MFCs) to an NCl_3 synthesis reactor. The resulting NCl_3 in chlorine gas is heated and goes to the temperature controlled NCl_3 destruction reactor. Finally, the gases are absorbed in a caustic scrubbing tank. The gases can be sampled at different points and passed through a sample bubbler containing concentrated HCl to collect any NCl_3.

The main system tubing was 1/4" O.D. and of 316 stainless steel. The sampling system, which operated at ambient temperature and close to atmospheric pressure, used 1/4" O.D. PFA (perfluoroalkoxy) tubing wrapped with aluminum foil to block UV light. The gases were metered into the system using mass flow controllers. Corrosion problems were encountered with corrosion of the stainless steel mass flow controllers being a particular problem. Problems like sticking or plugging were clearly indicated by an inability of the mass flow controller to maintain its set point. However, corrosion of the flowrate sensor components can lead non-obvious to flow errors. Because of this, the mass flow meter's needed periodic re-calibration (done by comparing air flow versus a rotameter before and after a test run). Most corrosion problems were due to the adsorption of moisture by the test system during maintenance and shutdowns, reducing the resistance of the stainless steel to later exposure to chlorine gas. Efforts were therefore made to keep maintenance periods short and to cap off any open lines during shutdowns.

The decomposition reactor consisted of a shell of 2.5" NPT (National Pipe Thread), Schedule 40, 316 stainless steel pipe, with a set of reducing couplings (2.5" NPT to 1" NPT then 1" NPT to ¼" NPT) at the inlet and outlet to provide a more smooth flow for the gas entering and exiting the reactor. The threaded connections were sealed with Teflon tape. This shell was heat traced to

maintain it at the target reaction temperature for the given test. Different liners made of 2" NPT Schedule 80 pipe (1.939" ID) could be used to change the reactor wall composition seen by the flowing gas. The stainless steel shell provided the capability to safely contain the chlorine gas when operating the destruction reactor at elevated temperatures and pressures. The small gap between the liner and the shell was sealed using flexible expanded-PTFE (polytetrafluoroethylene) joint sealant to prevent gases flowing in that area (Inertex UHF joint sealant). For most tests a PVDF (polyvinylidene difluoride) liner was used, while for some tests a 316 stainless steel liner was used. Two lengths of reactor were used, a 12" shell with a 13" liner (because the liner extends into the reducing couplings) and a 6" shell with a 7" liner. The line between the hot oil bath and the destruction reactor was insulated, but not heat traced. It was later thought that this may have introduced errors due to the tests being very temperature sensitive.

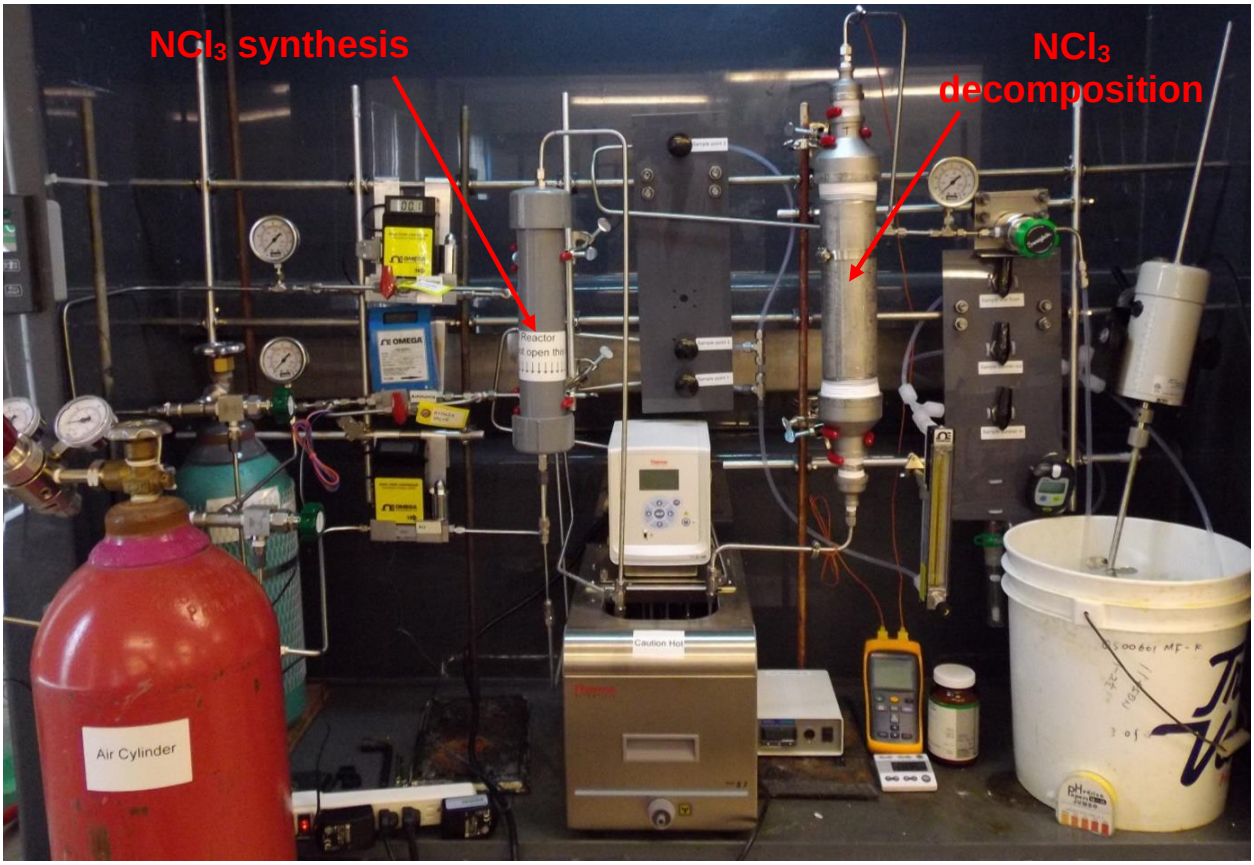

Figure 12: A photograph of the test system (before heating tape and insulation have been added).

8.2 NCl_3 synthesis

The NCl_3 synthesis reactor operated at ambient temperature and was made of 2" NPT, schedule 80, CPVC (Chlorinated PolyVinyl Chloride) piping components. The NCl_3 synthesis was done by adding a small flow of ammonia gas into a stream of chlorine. The NCl_3 is then generated by the reaction:

$$4\ NH_3(g) + 3\ Cl_2(g) \Rightarrow NCl_3(g) + 3\ NH_4Cl(s) + heat \qquad [17]$$

While this approach offers the direct production of a dry stream of chlorine containing NCl_3, it has been reported to be unreliable (26). One issue is the possible formation of intermediate products such as monochloramine and dichloramine which might lead to decomposition reactions. However, because this work was targeting low concentrations of NCl_3 in chlorine (<5000 ppmw), a large excess of chlorine is used. This factor, plus rapid mixing of the ammonia into the chlorine were hoped to be sufficient to drive the reaction to completion.

A second issue, which became apparent on testing initial synthesis reactor designs, was related to the co-production of solid ammonium chloride (NH_4Cl). Ammonium chloride is usually a very fine powder. The NH_4Cl produced by metering a small jet of ammonia into a main flow of chlorine was a combination of fine powder and an amorphous solid. The reaction was also extremely fast, resulting in solid amorphous NH_4Cl building up directly on the ammonia jet (ammonia flow ~25 cm/s). This problem has been described by others while trying to generate chloramine (39). Because this system had sufficient available ammonia pressure (typically 30-40 psi above the target system pressure) and the ammonia was fed using a mass flow controller that maintained a constant gas flow, the ammonia gas would force its way through the deposit. This resulted in the formation of further deposits in a manner that produced a growing tube of solid amorphous NH_4Cl (see Figure 13).

Figure 13: A tube of solid ammonium chloride growing from the ammonia gas inlet tube at the bottom of the picture. In this design, chlorine gas entered tangentially from the 1/8" tube at the left side and the growth of the solid NH_4Cl tube followed the spiral flow of the chlorine gas.

The formation of NCl_3 by this initial reactor design was also very erratic, with no NCl_3 formed at times during some test runs. Examination of the inside of the reactor found that for some of these runs, where the growing tube touched the CPVC reactor wall, there appeared to be localised melting of the CPVC indicating that the tip of the growing tube could be quite hot. As well as the heat from the synthesis reaction (equation 17), if the formed NCl_3 began to decompose, additional heat would be released (equation 2). Thus, it appeared that the local high temperature at the tip of the growing NH_4Cl tube could destabilize the forming NCl_3, which in turn would lead to further heat, intensifying the decomposition. Such a thermally driven auto-acceleration is likely the key factor in the unpredictable nature of the variations in the concentration of the synthesized NCl_3. This idea appears to be supported by the experience of Sisler et al (39) who worked to generate chloramine by mixing chlorine and ammonia gases. As well as solids build-up, they noted the mixing area could become quite warm and in some instances a yellow-white flame would appear and the chloramine yield would be very low. After trying different gas mixer arrangements and different gas mixtures, they noted that the total flow of gases was the most important factor, with a certain minimum flow required to achieve good product yields. This suggests that good heat removal is critical for the reactor operation.

After considering these issues, it was decided that a synthesis reactor design was required that maintained an unchanging environment around the tip of the growing NH_4Cl tube characterised by a high flow of gases to remove reaction heat. The resulting design involved directing the jet of ammonia gas into a long narrow tube filled with the flowing chlorine gas (see Figure 14). In this way, as the NH_4Cl tube grows, a strong and consistent flow of chlorine gas around the growing tube tip can be maintained (~50 cm/s). While this design greatly improved the reproducibility of the NCl_3 synthesis, variations still occurred. One cause is likely due to deposits of NH_4Cl powder in the tube altering the flow of chlorine around the tip of the growing NH_4Cl tube. The tubing was therefore arranged in a down-flow manner to discourage deposits of NH_4Cl powder. A second problem may be related to blocking of the end of the NH_4Cl tube, requiring the ammonia mass flow controller to deliver sufficient pressure to create a new opening, which would result in unsteady ammonia flow. A post-run image of an NH_4Cl tube inside the FEP tubing is shown in Figure 15.

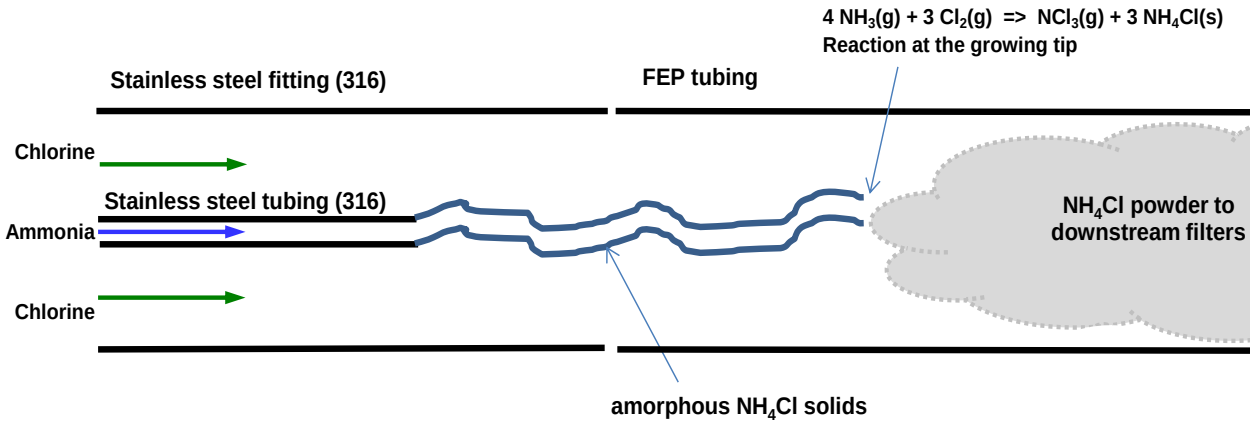

Figure 14: Gas phase reactor design to maintain good chlorine flow for heat removal at the growing tip of the NH_4Cl tube. Dimensions: ammonia feed 1/16" 316 tubing (0.022" I.D.) and the reactor of coiled 3/8" FEP (fluorinated ethylene propylene) tubing (1/4" ID).

A second issue with this approach to generating NCl_3 is the need to remove all NH_4Cl powder from the resulting NCl_3 and chlorine gas mix. As well as potentially fouling downstream surfaces,

it can interfere with the method used for NCl_3 analysis and generate a false reading. During initial troubleshooting of the synthesis reactor design, the synthesis reactor CPVC shell was temporarily replaced with transparent PVC to observe the growth of the NH_4Cl tube. During operation, the growing end of the NH_4Cl tube appeared to be giving off smoke, indicating the extremely fine size of the generated powder.

Figure 15: The post test run FEP tubing coil in a down-flow configuration inside the CPVC reactor body (the gases entered at the top right of the photo). After washing away the loose NH_4Cl powder outside and inside the FEP tubing, the NH_4Cl tube inside the FEP tube is visible.

The use of a 2” NPT pipe for the body of the synthesis reactor slowed the gas flow to ~1 cm/s to allow some settling of the NH_4Cl powder and provide more cross-sectional area for filtering. The primary filter, located about two thirds the way up the synthesis reactor, used two layers of 200 mesh 304 stainless steel cloth with an opening size of 0.003” (~76 µm). While this is a rather large opening, in use it was found to quickly build a filter cake that provided very good filtering. A second, similar filter at the outlet of the reactor collected only a small amount of powder, some of which had likely passed through the first filter before the filter cake was fully formed.

8.3 Analytical method

The analytical method involved bubbling a known volume of gas through concentrated HCl which can reactively absorb NCl_3 by converting it to ammonium. The HCl is then later analysed for ammonia to determine the NCl_3 in the gas stream. The method was developed from that recommended by EuroChlor for NCl_3 in liquid chlorine (40).

The gas sampling was controlled by opening a needle valve to draw the target flow from the sampling location through a rotameter to the gas bubbler (an ACE Glass 30 mL Midget Bubbler with a porosity A (145-175 µm) sintered glass bubbler). The PFA lines and the glass bubbler were covered with aluminum foil to prevent UV degradation of the NCl_3. The bubbler was filled with ~20 mL of concentrated HCl which will reactively absorb NCl_3 by converting it to ammonium:

$$NCl_3(g) + 4\ HCl(aq) \quad \Leftrightarrow \quad NH_4Cl(aq) + 3\ Cl_2(g) \qquad [18]$$

Where, concentrated HCl is used to ensure that the reaction equilibrium is driven far to the right. Once collected as ammonium chloride in HCl, the samples are stable and can be stored for later analysis. However, one can also see that any NH_4Cl powder that enters the bubbler will dissolve in the HCl and give a false NCl_3 reading. As a precaution against NH_4Cl powder, an in-line Tee-type particulate filter with a 0.5 µm pore size sintered stainless steel filter element (Swagelok SS-4TF-05) was used on the sampling line. Initially, two bubblers were used in series, but after it was found that essentially all the NCl_3 was being captured in the first bubbler, only one bubbler was used.

The collected samples were analysed using an ammonia electrode which measures ammonia gas crossing a hydrophobic membrane. This has the advantage of minimal interferences, but it requires that the ammonium be converted to ammonia. The collected samples are saturated with chlorine, which must first be removed to avoid reactions with ammonia. While the recommended method uses air sparging to accomplish the chlorine removal (40), in this work an excess of sodium sulphite (2.89 g per sample) was added to react any dissolved chlorine to chloride. Following the recommended method, the samples were then titrated to pH 7-7.5 with 25 wt% NaOH with care taken to use rapid stirring and to introduce the NaOH solution below the sample liquid level to avoid potential losses of ammonia gas. With care, the titration could be carried out to the target pH using 25 wt% NaOH alone without having to switch to a more dilute NaOH to avoid overshooting as is suggested in the EuroChlor method. It is thought that this is due to buffering by sodium bisulfite – sodium sulphite, which is present with our altered method. The samples were then made up to 100 mL with deionized water and allowed to cool to room temperature. Once at room temperature they were re-adjusted back to 100 mL.

Each batch of samples was split into two 50 mL portions to allow repeat measurements to be made. Just prior to analysis, 1 mL of 25 wt% NaOH was added to raise the pH and convert the aqueous ammonium to volatile ammonia for measurement. The measurements were made in a gently stirred beaker, with the ammonia electrode inserted through a LabWax cover to minimise any losses of ammonia vapour. Before and after each set of samples the electrode was re-calibrated to correct for electrode drift. Problems were initially encountered with excessive electrode drift and poor recovery from spiked samples. These problems were found to be due to the high ionic strength of our samples (41). To correct for this, the calibration standards were made starting from 200 mL of a high ionic strength solution containing 2.52 M NaCl plus 0.23 M Na_2SO_4 solution chosen to simulate the ion concentrations in the neutralised samples. This was spiked with 4 mL of 25 wt% NaOH to raise the pH and then specific volumes of ammonium standard were added from a burette to generate the calibration curve (similar to 40). The

electrode filling solution (0.1 M ammonium or 0.535 grams of NH_4Cl per 100 mL) was also adjusted by adding 4.25 g $NaNO_3$ per 100 mL to try to better match the osmotic pressures between the filling solution and the samples to decrease electrode drift (42). With this approach, standards made by spiking a known amount of ammonia standard solution into 20 mL of concentrated HCl, then following the sample work-up, gave recoveries of 1.04 +/- 0.13.

While the system ran reasonably well, the results were not as reliably steady as was wished. Because of this, each test run was run at one test condition with repeated alternate samples taken at the NCl_3 destruction reactor inlet and outlet to provide an average measure of the NCl_3 decomposition. The results from an example test run are shown in Figure 16. Each sample was taken for 16 minutes and involved diverting about 40% of the total system gas flow through the sampling system. If there was any significant amount of powder in the sampling system, it would have made it difficult to measure the low NCl_3 concentrations shown at the decomposition reactor outlet in Figure 16.

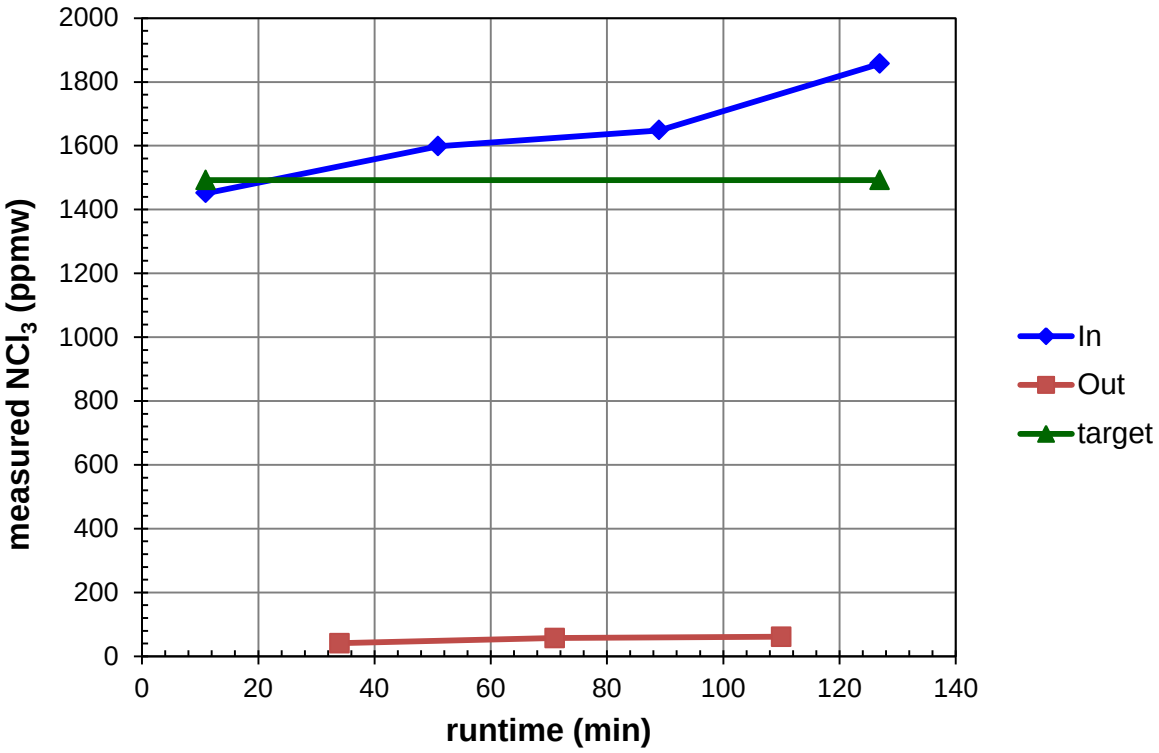

Figure 16: Inlet and outlet NCl_3 concentrations and measurement times. Decomposition reactor 70°C, 5 psig and residence time of ~41 s. Target value is the expected value based on the MFC settings.

9. Results

The experimental results consist of data similar to that shown in Figure 16. This means that for each test condition one obtains an inlet concentration, an outlet concentration and a residence time. The ability to measure the reaction extent is limited by the measurement range of the ammonia electrode. Because it works on a logarithmic scale, it is difficult to accurately measure small differences between the decomposition reactor inlet and outlet concentrations. For

example, if the minimum clearly distinguishable change in the electrode output is 5 mV, this corresponds $C_{out}/C_{in} = 10^{(-5/58.2)} = 0.82$ (for an electrode slope of 58.2 mV/decade for measurements at 20°C). Thus, the minimum detectable amount of reaction would be ~18% of the feed concentration. At the other extreme, blanks were measured at 0.5 +/- 0.3 ppm and, after work-up, our ammonia concentrations for the reactor inlet samples were around 50 ppm for typical test runs. This means that the lowest detectable C_{out}/C_{in} ~ 0.8/50 = 0.015 and so the maximum quantifiable amount of reaction would be ~98.5% of the feed concentration.

9.1 Kinetic measurements

Initial testing focused on measuring the effect of temperature on the NCl_3 decomposition reaction. To minimize possible wall effects, for these tests the decomposition reactor was operated with a PVDF liner. The PVDF liner was chosen because similar plastic surfaces (Teflon) have been reported to be less active than metal surfaces for quenching chlorine atom radicals (43).

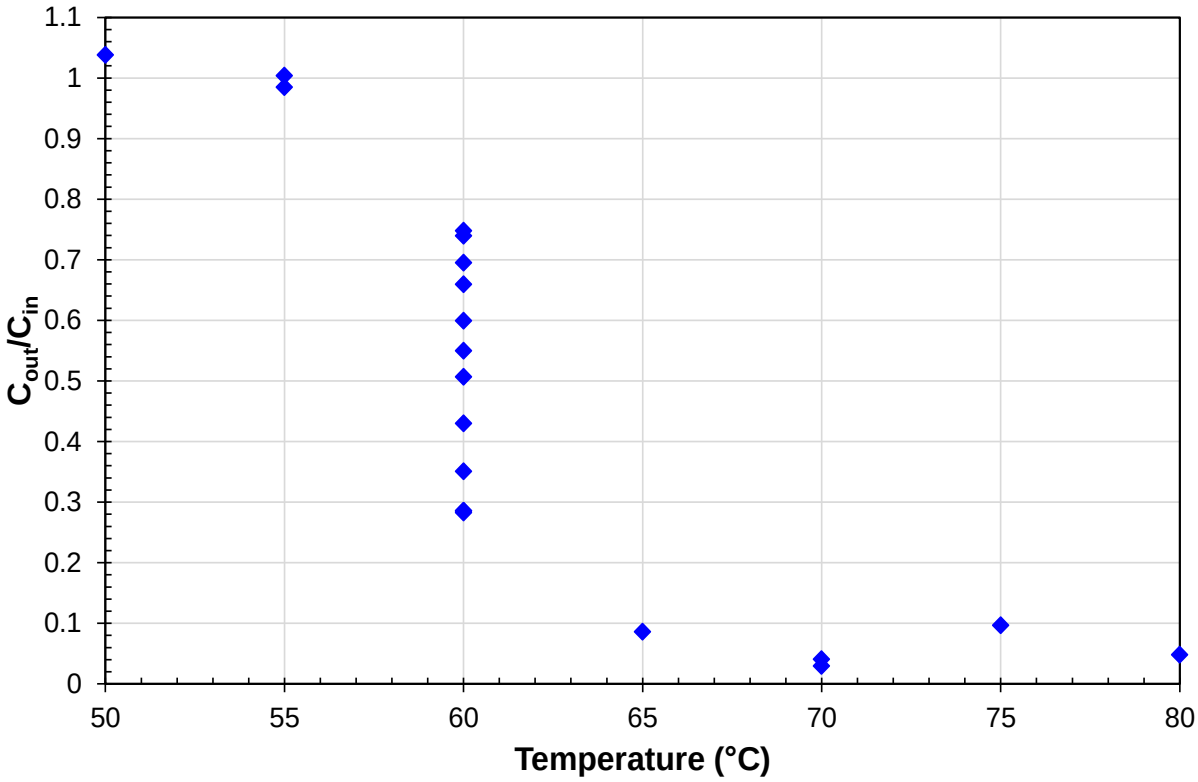

Figure 17: C_{out}/C_{in} values as a function of temperature. Conditions: PVDF lined decomposition reactor, total pressure 1.36 to 2.25 bara, C_{in} 1280 to 2215 ppmw NCl_3, and residence time 41 to 137 s.

These initial tests found that rather than a smooth increase of reaction rate with temperature, there appeared to be an abrupt turn-on (see Figure 17). Over a 10°C range, from 55°C to 65°C the rate goes from no detectable reaction to close to complete reaction. These results are not entirely unexpected since the decomposition of NCl_3 is autocatalytic as is shown by its ability to spontaneously detonate under some conditions. However, at the above ambient pressures used in these tests it had been anticipated that chain branching reactions would be suppressed, and

the reactions might behave in a manner more like the apparent first order decomposition reported in liquid chlorine.

This autocatalytic behaviour raised issues for trying to obtain good data. The extreme sensitivity of the reaction rate to temperature means that even very small temperature variations can result in significant changes in extent of reaction for a given residence time. This was especially true around 60°C where the reaction is rapidly accelerating. This can be seen in Figure 18 in the large scatter in C_{out}/C_{in} values all taken at nominally 60°C based on the decomposition reactor temperature controller setting.

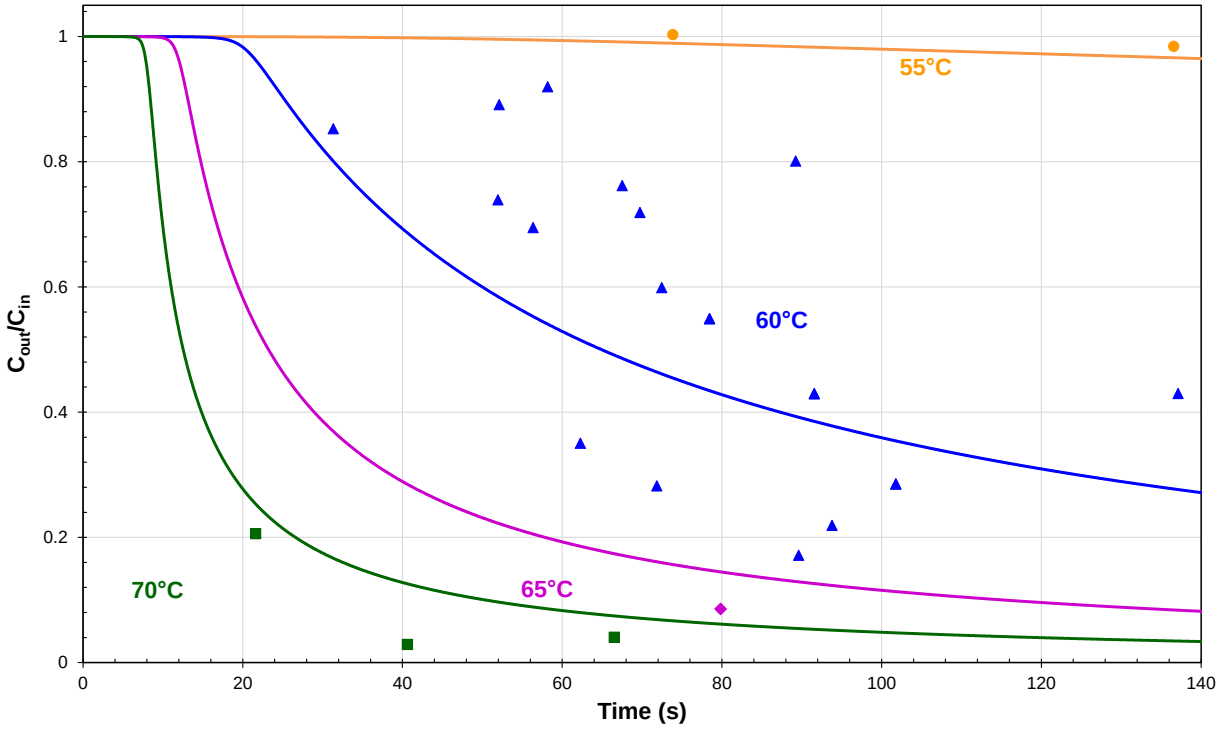

Figure 18: C_{out}/C_{in} values for different temperatures as a function of retention time. Conditions: PVDF lined decomposition reactor, total pressure 1.36 to 2.25 bara and C_{in} 1364 to 2863 ppmw NCl_3. Curves from the model discussed in Section 10.

In Figure 18, data is shown at different temperatures and for different decomposition reactor residence times, where the gas flow rate was changed to obtain the different residence times. One can again see the huge increase in rate on simply changing from 55°C to 65°C. Based on the previous literature, the reactions of NCl_3 are also expected to be pressure sensitive. However, if the data at 60°C is separated into different pressures and re-plotted as shown in Figure 19, no clear pressure dependence is visible. A key issue is that changing gas flow rates or system pressures can influence system heat transfer and heat loss characteristics and so the results may include a temperature variation effect even if the nominal test temperature, as set by the decomposition reactor shell temperature controller, is unchanged.

Finally, because of the multiple and interacting reaction steps, autocatalytic reactions cannot be simply described by a single rate constant for a single rate determining step. Therefore, only measuring the reactor inlet and outlet concentrations for a given set of conditions will indicate how much decomposition can be achieved under those particular conditions but will give little

information about the detailed reaction mechanism and kinetics. This makes it difficult to use the obtained data to predict performance under other conditions without employing a model of the autocatalytic reactions.

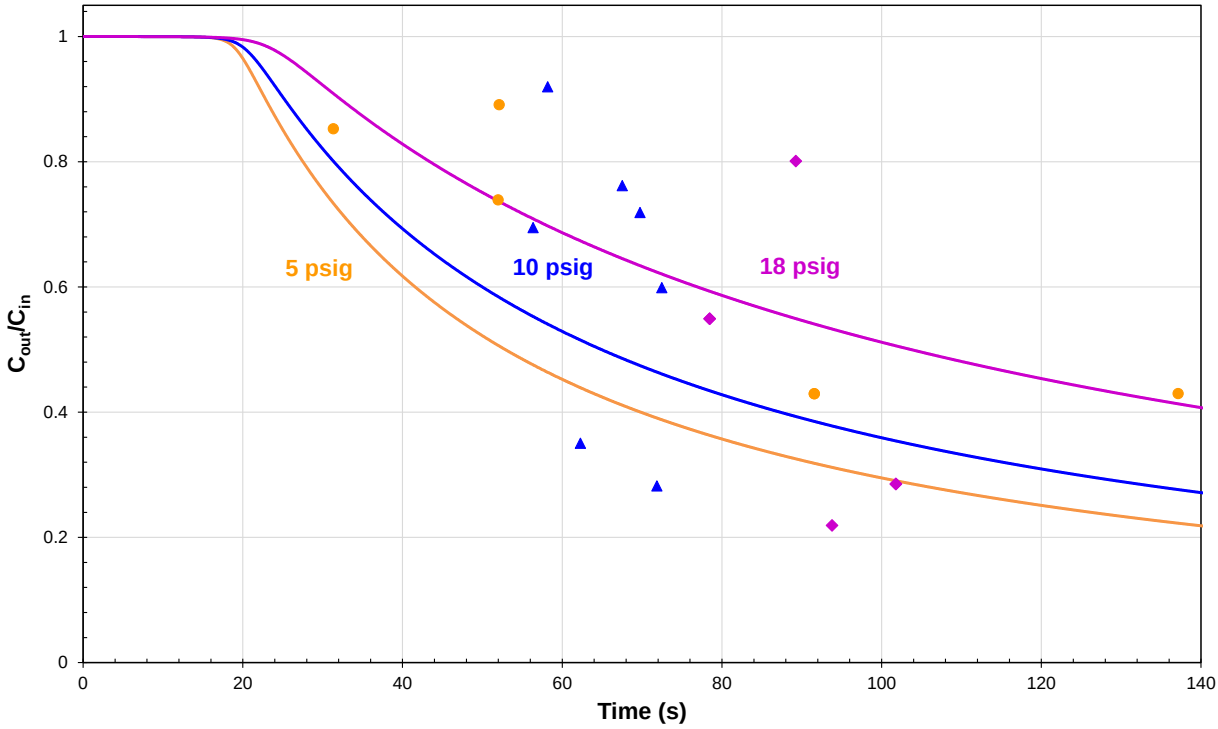

Figure 19: C_{out}/C_{in} values for different pressures as a function of retention time. Conditions: PVDF lined decomposition reactor, 60°C and C_{in} 1364 to 2863 ppmw NCl_3. Curves from the model discussed in Section 10.

9.2 Reactor surface effects

Testing was also done to see the effect of different decomposition reactor liners. As was discussed earlier, metal surfaces are reported to quench chlorine atom radicals more than Teflon (43). To try to see any effect, repeat runs were done with the PVDF liner, then a 316 stainless steel liner, and then a repeat set of runs with the PVDF liner. The results of these tests are shown in Figure 20. The metal liner appears to result in slightly less NCl_3 decomposition, though the effect is not large.

Note that the metal surfaces, after exposure to dry chlorine gas are typically covered by a layer of anhydrous metal chlorides (17). Also, both surfaces may have some contamination by traces of NH_4Cl powder escaped from the NCl_3 synthesis. Surfaces covered with salts tend to be less active than metals for chlorine atom recombination, but more active than plastics like Teflon (43,44). However, while the metal surface in these tests might be less active than a clean metal surface, they would be more representative of the passivated metal surfaces in industrial dry chlorine service. Note that for industrial applications a reactor vessel would be much larger and so have a smaller surface area to volume ratio, thus, these surface effects would be less

important. Though, wall effects have been reported to slow the UV driven decomposition of NCl_3 in an industrial pipe reactor in areas roughly within an inch or two of the pipe wall (45).

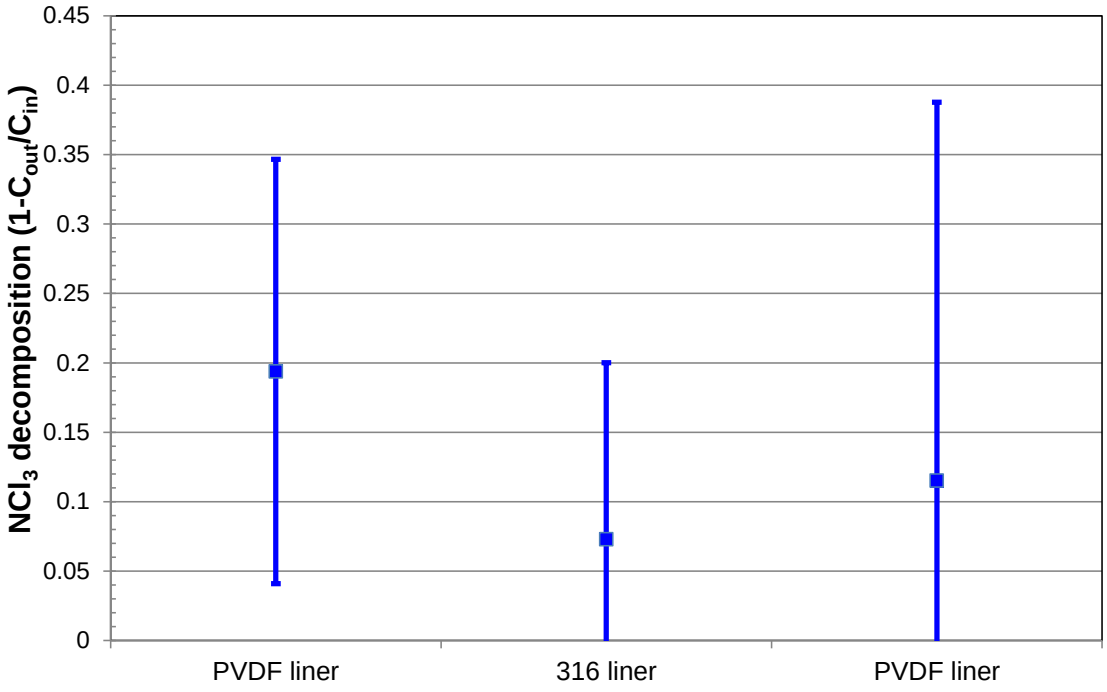

Figure 20: Results for NCl_3 decomposition in the decomposition reactor run with different liners (PVDF = polyvinylidene difluoride and 316 = alloy 316 stainless steel). Decomposition reactor at 60°C, system pressure 10 psig, Cin 1200-3200 ppmw, and retention times 55-70 s. Plot shows averages and one standard deviation for 8 data points (PVDF), 9 data points (316) and 6 data points (PVDF repeat).

As an extreme case, the reactor, using the PVDF liner was filled with two Monel knitted wire mesh pads (2" OD x 6" tall Monel catalyst pads made of knitted wire mesh from Metal Textiles of Edison, NJ)(see Figure 21). Prior to use, the mesh pads were degreased with acetone and air dried. Once installed in the decomposition reactor, the Monel was exposed to chlorine gas flow and slowly heated to 60°C to ensure the metal surface was stable under the target test conditions. Testing was then carried out with the decomposition reactor in this configuration.

The testing results found that the presence of the Monel pads significantly inhibited the reaction. In fact, it required heating the decomposition reactor to ~75°C to obtain the NCl_3 decomposition rate found in the empty reactor at 60°C. These results are consistent with the results of Clark and Clyne where they used a nickel wire to remove atomic chlorine radicals and demonstrate their importance in the reaction mechanism (31).

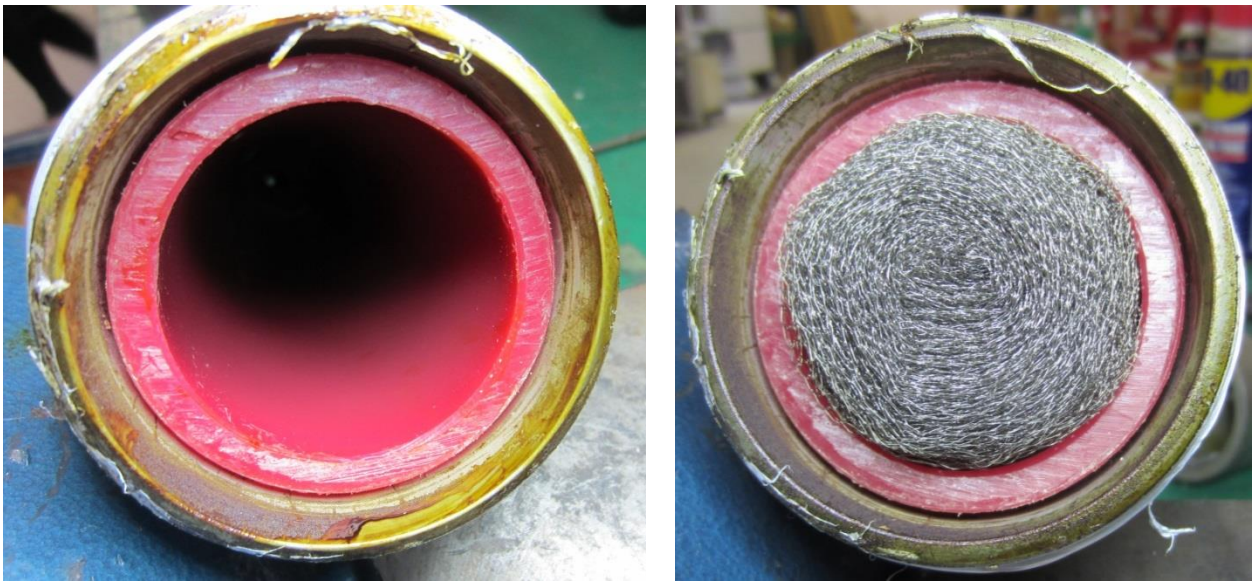

Figure 21: The NCl_3 destruction reactor with a PVDF liner, shown empty and loaded with the Monel mesh pads.

9.3 Local hot-spot testing

It has been reported that NCl_3 can be decomposed by the gas heating occurring during gas compression (13). However, insufficient information was provided to determine kinetics. Different results have also reportedly been found at different facilities with different compressor maximum temperatures, possible addition of holding pipes to keep the gas at temperature for longer periods, and different flow geometries and exposed surfaces all possibly playing a role (17). One question raised by these inconsistent results is the possibility that a local hot spot in the chlorine flow might be able to initiate NCl_3 decomposition.

To test this idea, a small heater was used to generate a hot spot in the entrance area of the decomposition reactor. This heater is shown in Figure 22. A small Incoloy shell, ¼" cartridge heater with an internal thermocouple was used to generate a controlled temperature hot spot. The cartridge heater was inserted through a small piece of 40 mesh Nichrome screen to improve the heat transfer to the gas flow. The use of high nickel alloy materials was done to avoid the danger of a chlorine fire.

The tests were done with the decomposition reactor at ambient temperature (22-25°C), a system pressure of 10 psig, and C_{in} 1300-2200 ppmw with a gas residence time in the decomposition reactor of ~62 s. Without the heated screen, at ambient conditions there was no measurable difference between the decomposition reactor inlet and outlet NCl_3 concentrations. With the screen heated at 160°C, the NCl_3 decomposition ($1 – C_{out}/C_{in}$) was 0.11 +/- 0.12. In a second run with the screen temperature raised to 200°C, the NCl_3 decomposition was 0.58 +/- 0.04. And so, even with the tip of the cartridge heater at 200°C, the presence of a local hot spot was not able to initiate a self-sustaining decomposition that could completely react the NCl_3. This is not entirely surprising, since at the pressures used in this work and a maximum NCl_3 concentration of ~0.13 mole%, we are far above the pressure range where the reaction is reported to self-propagate (see Figure 10).

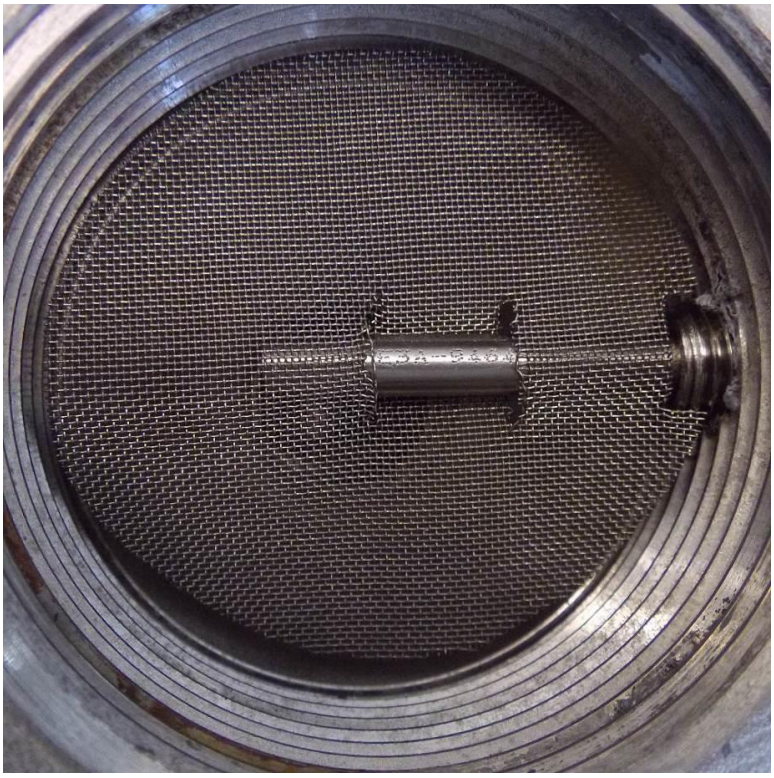

Figure 22: Local hot spot testing using a temperature controlled cartridge heater to heat a metal screen located in the mouth of the decomposition reactor. The cartridge heater shell and the metal screen were both of high nickel alloys.

9.4 Effect of other gases

Testing was also done to see the possible influence of the presence of other gases. In these tests a third mass flow controller was used to mix air (Praxair Ultra Zero, <2 ppm water and <0.1 ppm total hydrocarbons) or nitrogen (Praxair Ultra High Purity, <1 ppm oxygen, <3 ppm water and <0.5 ppm total hydrocarbons) into the chlorine flow ahead of the NCl_3 synthesis reactor. The total volume flowrate was kept the same to maintain the residence time in the decomposition reactor at 59 to 72 s. Three tests were carried out using: 25 mole% air, 26 mole% nitrogen and 31.5 mole% air. The results of these tests did not show any significant different in NCl_3 decomposition rate versus reference tests with pure chlorine.

Other tests were carried out where bromine (a common trace contaminant of chlorine) was added to the gas flow. To accurately add a trace amount of bromine to the gas stream, a small metered air flow was bubbled through room temperature liquid bromine. This produced a flow of essentially bromine saturated air that was then added to the chlorine-NCl_3 gas flow after the first set of filters in the NCl_3 synthesis reactor (see Figure 11). The amount of bromine used was determined by weighing the bubbler before and after the experiment.

Two separated test runs were carried out using 1700-2500 ppmw NCl_3, 2600-3200 ppmw Br_2, a system pressure of 10 psig, a decomposition reactor temperature of 60°C, and residence times of 61-65 s. Reference runs were also done using 1400-2500 ppmw NCl_3 and decomposition reactor residence times of 62-72 s. The results from the two sets of tests were not significantly

different and so with our test setup at the conditions tested, no effect of bromine on the NCl_3 decomposition could be seen.

10. Discussion

As mentioned previously, because of the complexity of the autocatalytic reactions involved, it is difficult to understand the obtained data without employing a model of the reactions.

10.1 Reaction steps

The reactions of NCl_3 decomposition involve a range of different intermediates and numerous possible reaction steps have been suggested. However, for this work, using information from the literature a simple mechanism is described that can capture the main reaction trends reported in the literature and quantitatively fit the results observed in this work.

The NCl_3 is diluted in a large excess of chlorine and chlorine atoms are involved in the reaction and so the reactions of chlorine were first considered. The thermal dissociation of chlorine is a pressure sensitive, 2nd order reaction (46,47).

$Cl_2 + M' \Leftrightarrow 2\,Cl^* + M$ [Step 1f]

Where M' is a gas molecule that transfers energy to the chlorine and the rate constant reported to be: $k_{1f} = 8.49x10^{15} \exp(-E_a/RT)\ cm^3mole^{-1}s^{-1}$. The activation energy (E_a) is 233.7 kJ/mole (48), which is very close to the chlorine-chlorine bond energy of 239.7 kJ/mole (49). The reverse reaction is:

$2\,Cl^* + M \Leftrightarrow Cl_2 + M'$ [Step 1r]

Where, in this case, the other gas molecule absorbs energy from the activated complex formed by the collision of two chlorine atoms allowing it to stabilize as a chlorine molecule. The rate constant is reported to be: $k_{1r} = 1.26x10^{15} \exp(-E_a/RT)\ cm^6mole^{-2}s^{-1}$ for M = Cl_2 and here E_a = -6.7 kJ/mole (50). However, at the pressures and temperatures being considered in this work, the equilibrium amount of atomic chlorine will be quite small. The main source of free radicals is thought to be from the thermal dissociation of NCl_3 (27).

$NCl_3 + M' \Leftrightarrow NCl_2^* + Cl^* + M$ [Step 2]

Similar to chlorine dissociation, this can be written as a pressure sensitive reaction. Using a Lindemann approach (51) the reaction can be written in steps.

$NCl_3 + M' \Leftrightarrow NCl_3' + M$ [Step 2a]

$NCl_3' \Leftrightarrow NCl_2^* + Cl^*$ [Step 2b]

And so, the effective reaction rate constant is given by:

$$k_{2f} = \frac{k_{2af}k_{2bf}[M]}{k_{2ar}[M]+k_{2bf}} \quad [19]$$

Where, the activation energy should roughly equal the energy to break the NCl_2-Cl bond. The bond energy of NCl_2-Cl has been approximately estimated to be 96±58 kJ/mole (1±0.6 eV) (32). At low pressures (low [M]) the rate constant would approach:

$$k_{2f} \rightarrow k_{2f0}[M] \approx k_{2af}[M] \quad [20]$$

While at high pressures (high [M], P → ∞) the rate constant would approach:

$$k_{2f} \rightarrow k_{2f\infty} \approx \frac{k_{2af}k_{3bf}}{k_{2ar}} \quad [21]$$

The reverse reaction would also be pressure sensitive (as suggested by (31)) and would be given by:

$$k_{2r} = \frac{k_{2ar}k_{2br}[M]}{k_{2ar}[M]+k_{2bf}} \quad [22]$$

At high pressures this reaction would become:

$$k_{2r} \rightarrow k_{2r\infty} \approx k_{2br} \quad [23]$$

This shifting rate of Step 2 with pressure is likely important for the low pressure behaviour of NCl_3 decomposition reported in the literature (discussed in Section 7). However, for this work at above ambient pressure, only the high pressure limits will be used. The reverse reaction is also reported to be in competition with (31):

$NCl_2^* + Cl^* \Rightarrow NCl + Cl_2$ [Step 3]

The rate constant for this reaction is reported to be: $k_3 = 3.98 \times 10^{12} \exp(-E_a/RT)$ $cm^3mole^{-1}s^{-1}$ with E_a = 12.89 kJ/mole (32).

Once atomic chlorine has been formed in Step 2 it can react with NCl_3 (31,32):

$Cl^* + NCl_3 \Rightarrow NCl_2^* + Cl_2$ [Step 4]

With an estimated value of $k_4 = 2.0 \times 10^{12}$ $cm^3mole^{-1}s^{-1}$ at 25°C as discussed in Section 7. The reaction of NCl_2^* is thought to produce a combination of chlorine atoms and excited chlorine molecules, where some workers speculate that the excited chlorine molecules can later dissociate to give further chlorine atoms (52,53). The overall reaction can be summarized as:

$2\ NCl_2^* \Rightarrow N_2 + n\ Cl^* + (2\text{-}n/2)\ Cl_2$ [Step 5]

Where n could potentially vary from 0 to 4 (from quenching to rapid acceleration). As discussed previously, the rate of acceleration of the decompositions reactions, as measured by explosive limits (27), flame speeds (19) and UV light quantum efficiencies (30) is very sensitive to the total system pressure. This indicates that pressure influences the chain branching in Step 5 and so the value of n. Step 5 is also thought to give rise to excited chlorine molecules that are responsible for the observed chemiluminescence.

For this work a simplified model is used for Step 5 that assumes high energy intermediates in the reaction chain that can either transfer energy to surrounding molecules through collisions or

release atomic chlorine. For this approach, Step 5 is subdivided into two steps with two transient intermediates (N_2Cl_4' and N_2Cl_2'), each which can react through pathways that depend on pressure.

$2\ NCl_2^* \quad \Rightarrow \quad N_2Cl_4'$ [Step 5a]

With $k_{5a} = 5.01x10^{11}\ cm^3mole^{-1}s^{-1}$ and $E_a \approx 0$ (32). Where, the resulting intermediate can react in two possible ways.

$N_2Cl_4' + M \quad \Rightarrow \quad N_2Cl_2' + M' + Cl_2'$ [Step 5b]

$N_2Cl_4' \quad \Rightarrow \quad N_2Cl_2' + 2\ Cl^*$ [Step 5c]

This is then followed by:

$N_2Cl_2' + M \quad \Rightarrow \quad N_2' + M' + Cl_2'$ [Step 5d]

$N_2Cl_2' \quad \Rightarrow \quad N_2' + 2\ Cl^*$ [Step 5e]

This mechanism results in an n value for overall the reaction in Step 5 that varies from 0 to 4 as a function of pressure. The observed light emission during NCl_3 decomposition would then be related to the relaxation of the Cl_2' (Steps 5b and 5d). This is likely a simplification and these reactions may not be correct, but it is hoped that they lead to an approximately correct mathematical form.

A reaction of NCl_2^* with NCl_3 has also been suggested (27,36), though Clark and Clyne found the reaction undetectable under their conditions (32). It was therefore decided, in the interest of simplicity, to only include the presumably more dominant reaction of Step 5.

Using the above equations, the production of atomic chlorine from N_2Cl_4' would be given by:

$$rateCl*_{5c} = 2rate_{5a}\frac{k_{5c}}{k_{5c}+k_{5b}[M]} \quad [24]$$

Where at low [M] each N_2Cl_4' would yield 2 chlorine atoms, while at high pressures the yield would drop to zero. Following the Lindemann model, the area where this shift in pathways occurs is called the fall off region (51). However, the reaction as written in equation 25 is a simplification because the surrounding molecular energies and the collision induced energy transfers will not be single valued. Because of this, the transition between the two pathways will not be as abrupt as predicted using equation 24. A number of sophisticated models have been developed to correct the Lindemann model using a correction factor (F).

$$rateCl*_{5c} = 2rate_{5a}\frac{k_{5c}}{k_{5c}+k_{5b}[M]}F \quad [25]$$

These typically require a number of fitting parameters that must be obtained by fitting large data sets or be estimated from first principles. However, a simple, approximate correction can be made using (54):

$$F \approx 0.6^{\left[1+\left(log(P_R)\right)^2\right]^{-1}} \quad [26]$$

Where P_R is the reduced pressure, which is equal to the system pressure divided by the fall-off pressure ($P_R = P/P_{1/2}$). The fall-off pressure is related to the concentration of the surrounding molecules (in this case essentially chlorine molecules) at which the two reaction pathways (5b and 5c) are in balance:

$$\frac{P_{1/2(5bc)}}{RT} = [M]_{1/2(5bc)} = \frac{k_{5c}}{k_{5b}} \quad [27]$$

And so:

$$rateCl*_{5c} = 2rate_{5a} \frac{1}{1+{}^{P}/_{P_{1/2(5bc)}}} 0.6^{\left[1+\left(log\left({}^{P}/_{P_{1/2(5bc)}}\right)\right)^2\right]^{-1}} \quad [28]$$

This then gives the n in equation 5 as:

$$n = \frac{2}{1+{}^{P}/_{P_{1/2(5bc)}}} 0.6^{\left[1+\left(log\left({}^{P}/_{P_{1/2(5bc)}}\right)\right)^2\right]^{-1}} + \frac{2}{1+{}^{P}/_{P_{1/2(5de)}}} 0.6^{\left[1+\left(log\left({}^{P}/_{P_{1/2(5de)}}\right)\right)^2\right]^{-1}} \quad [29]$$

Where at low pressures ($P \rightarrow 0$), this will give an n approaching 4, while at high pressures ($P \rightarrow \infty$), the predicted n approaches 0.

And finally, reaction 3 is linked back into the model by:

2 NCl ⇨ N_2Cl_2' [Step 6]

With a rate constant at 25°C estimated to be: $k_6 \geq 2.0 \times 10^{12}$ $cm^3 mole^{-1} s^{-1}$ (32).

10.2 Model fitting

To incorporate the reaction steps into a practical model, constants need to be estimated for reaction steps where kinetic data is not available and assumptions are made to simplify the calculations. One assumption is that the high energy intermediates in Step 5 rapidly reach a pseudo steady-state, then:

$$\frac{d[N_2Cl_4\prime]}{dt} = rate_{5a} - rate_{5b} - rate_{5c} \approx 0 \quad [30]$$

$$\frac{d[N_2Cl_2\prime]}{dt} = rate_6 + rate_{5a} - rate_{5d} - rate_{5e} \approx 0 \quad [31]$$

The approach to estimating the degree of chain branching involved fitting data from the work of Griffiths and Norrish (30), where UV light was used to initiate a slow decomposition of NCl_3 in Cl_2. The initiation reaction was given in equation 11.

Cl_2 + hv ⇨ 2 Cl* [Step 0]

In their experiments, the method of initiating the reaction by UV light would be more significant than thermal initiation at ambient temperatures and so, for their work, Steps 1 and 2 can be ignored. In their work, the reaction was driven slowly over 200-1000 s and so the concentrations of Cl* and NCl_2* are expected to be small and so Step 3 will also be ignored. Thus, for their test conditions, we can consider the primary reactions to be Steps 0, 4 and 5. Then, with the slowly driven reaction, assuming the reactive intermediates quickly reach pseudo steady-state gives:

$$\frac{d[Cl*]}{dt} = 2h\nu - k_4[NCl_3][Cl*] + nk_5[NCl_2*]^2 \approx 0 \quad [32]$$

$$[Cl*] = \frac{2h\nu + nk_5[NCl_2*]^2}{k_4[NCl_3]} \quad [33]$$

And:

$$\frac{d[NCl_2*]}{dt} = k_4[NCl_3][Cl*] - 2k_5[NCl_2*]^2 \approx 0 \quad [34]$$

Using equation 34 to eliminate [NCl_2*] from equation 33 gives:

$$[Cl*] = \frac{h\nu}{k_4[NCl_3]}\left(\frac{4}{2-n}\right) \quad [35]$$

Note that pseudo steady-state cannot occur (i.e. the system is inherently unstable) unless n < 2. In this slow, steady NCl_3 consumption condition, the rate of NCl_3 disappearance would be approximately given by:

$$\frac{d[NCl_3]}{dt} \approx -k_4[NCl_3][Cl*] = -h\nu\left(\frac{4}{2-n}\right) \quad [36]$$

In their paper, Griffiths and Norrish measured the quantum efficiency for NCl_3 removal (ε = NCl_3 removed per light quanta).

$$\varepsilon = \frac{-\frac{d[NCl_3]}{dt}}{h\nu} \quad [37]$$

Then, using equations 29, 36 and 37 and writing in terms of the fall-off pressures gives:

$$\varepsilon = \frac{4}{2-\left(\frac{2}{P/P_{1/2(5bc)}+1}0.6^{\left[1+\left(log\left(P/P_{1/2(5bc)}\right)\right)^2\right]^{-1}} + \frac{2}{P/P_{1/2(5de)}+1}0.6^{\left[1+\left(log\left(P/P_{1/2(5de)}\right)\right)^2\right]^{-1}}\right)} \quad [38]$$

Griffiths and Norrish measured quantum efficiencies over a range from 30 to 940 mbara total pressure for NCl_3 in chlorine and other gases and found a relationship roughly approximated by equation 13. Their results can also be fit by equation 38. Their data is plotted in Figure 23 along with a best fit curve using equation 38 with p_{5bc} = 4.3 mbara ($[M]_{1/2}$ = 1.7x10^{-7} mole/cm^3) and p_{5de} = 612 mbara ($[M]_{1/2}$ = 2.5x10^{-5} mole/cm^3). Note that mathematically the two fall-off pressures could equally well be reversed. It is also interesting to note in Figure 23 that at 25°C

and 940 mbara (hence close to ambient conditions), the quantum efficiency is still greater than 2 implying an n > 0 and so some level of chain reactions still occurring.

The temperature dependence of these fall-off pressures would be given by the activation energy difference between the two competing reactions. For example, $P_{1/2(5bc)} = k_{5c}/k_{5b}$. The activation energy for the energy transfer collision (Step 5b) is generally assumed to be zero (51) and so the temperature dependence of $P_{1/2(5bc)}$ would be equal to the activation energy of Step 5c. The initial step in Step 5c might be expected to be:

$N_2Cl_4' \Rightarrow N_2Cl_3^* + Cl^*$ [39]

And so, the activation energy would likely be similar to the energy to break the nitrogen-chlorine bond (Cl_2NNCl-Cl). In an analogous manner, the temperature dependence of $P_{1/2(5de)}$ would be similar to the activation energy associated with breaking the first nitrogen chlorine bond in N_2Cl_2' (ClNN-Cl). These bond energies are not known, but the bond energies of similar bonds in NCl_3 have been roughly estimated (Cl_2N-Cl ≈ 96 kJ/mole and ClN-Cl ≈ 145 kJ/mole (32)). These values were only rough estimates and the bonds in question are different, but these values can be used as a starting point for fitting the temperature dependences of the fall-off pressures in the model.

For $k_{2f\infty}$ and k_{2r} there are 2 activations energies and 2 pre-exponential factors to be fitted. The absorption of energy by collision with a gas molecule (Step 2br) is assumed to have no activation barrier and so $E_{A2br} \approx 0$ (51). The activation energy for the initial dissociation of NCl_3 might be expected to be close to the energy to break the Cl_2N-Cl bond. This bond energy was roughly estimated to be around 96±58 kJ/mole (32). For Step 4 the activation energy is not known, however the activation energy for Step 3 is reported as E_a = 12.9 kJ/mole (32). The removal of the first chlorine (Step 4) was assumed to be easier and so an initial guess for the activation energy for Step 4 of ~9 kJ/mole was chosen.

The model was then fit to the data from this work which resulted in the values listed in Table 3. Note that the fitted values were obtained by fitting the limited and somewhat noisy data obtained in this work and so should be used with caution, though many of the fitted values are not far from the initial estimated guesses, suggesting that they are reasonably correct.

The ability of the model to fit the measured data can be seen in Figures 18 and 19. The fitting can be improved and the reaction mechanisms, especially related to Step 5, are a simplification, but the limited extent of available data and its uncertainty restricts the ability to develop a more complex model. However, it is hoped that the key dominant reactions and trends have been captured by this model. As discussed earlier, extending the model to lower pressures would require a more complete fit of the sub-steps of Step 2 (four additional constants).

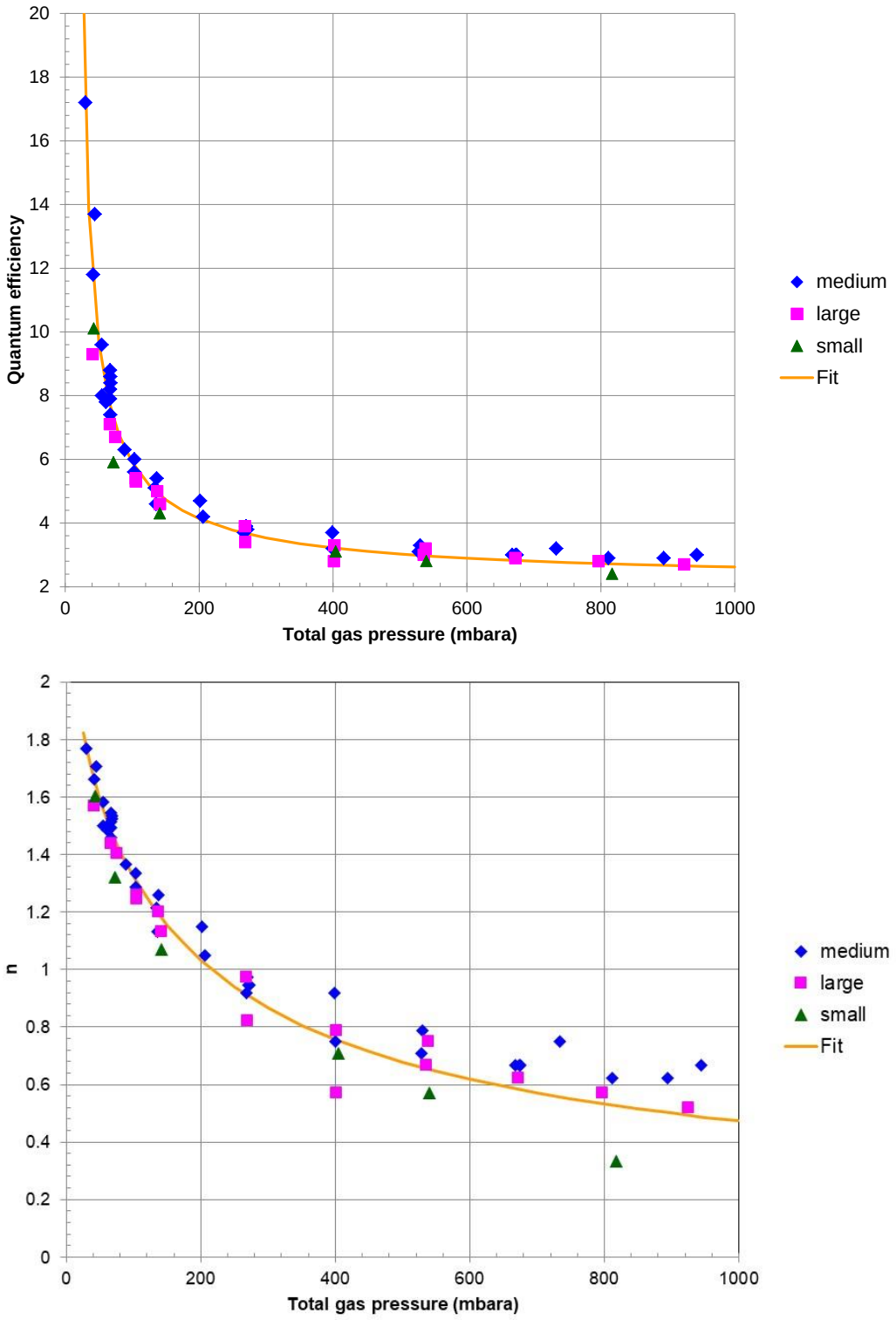

Figure 23: Top: Quantum efficiency for decomposition of NCl_3 versus pressure for three different geometries of vessels from (30). Bottom: the implied values for n for the data. The fitted curves were found using equation 38.

Table 3: The constants used for the model

Constant	Pre-exponential	Activation energy (E_a) kJ/mole	Remarks
k_{1f}	8.49×10^{15} $cm^3 mole^{-1} s^{-1}$	233.7	Ref. 48
k_{1r}	1.26×10^{15} $cm^6 mole^{-2} s^{-1}$	-6.7	Ref. 50
$k_{2f\infty}$	2.8×10^{7} $cm^3 mole^{-1} s^{-1}$	85.5	fitted
k_{2r}	2.4×10^{14} $cm^6 mole^{-2} s^{-1}$	~0	fitted pre-exponential and assumed E_a
k_3	3.98×10^{12} $cm^3 mole^{-1} s^{-1}$	12.9	Ref. 32
k_4	2.0×10^{12} $cm^3 mole^{-1} s^{-1}$ (at 25°C)	12.6	pre-exponential based on 32 and fitted E_a
k_{5a}	5.01×10^{11} $cm^3 mole^{-1} s^{-1}$	~0	Ref. 32
k_{5b}/k_{5c}	$P_{1/2(5bc)}$ = 4.28 mbara at 25°C	116	Fall off pressure fitted to Ref. 30 and E_a fit using this work
K_{5d}/k_{5e}	$P_{1/2(5de)}$ = 610.4 mbara at 25°C	149	Fall off pressure fitted to Ref. 30 and E_a fit using this work
k_6	2.0×10^{12} $cm^3 mole^{-1} s^{-1}$	0	Ref. 32

Based on the reaction steps discussed above, the model would predict the rate of NCl_3 decomposition to be given by equation 40 (for ambient and higher pressures).

$$\frac{d[NCl_3]}{dt} = -k_{2f\infty}[NCl_3] + k_{2br}[NCl_2*][Cl*] - k_4[NCl_3][Cl*] \quad [40]$$

The first term is the initial thermal decomposition of NCl_3. The estimated rate of this reaction was substantially higher than Step 1, and so to simplify the calculations Step 1 was not included in the final model. Similarly, under the conditions covered in this work, the rate of Step 3 and so also Step 6 were much smaller than the other steps and so they were also not included in the final model.

This initial decomposition reaction is then accelerated by the radical chain reactions involving Cl* and NCl_2*. The related equations for the radical species are given in equations 41 and 42.

$$\frac{d[Cl*]}{dt} = k_{2f\infty}[NCl_3] - k_{2br}[NCl_2*][Cl*] - k_4[NCl_3][Cl*] + nk_{5a}[NCl_2*]^2 \quad [41]$$

$$\frac{d[NCl_2*]}{dt} = k_{2f\infty}[NCl_3] - k_{2br}[NCl_2*][Cl*] + k_4[NCl_3][Cl*] - 2k_5[NCl_2*]^2 \quad [42]$$

A key factor in the degree of acceleration of the decomposition reactions is the value of n, which is given by equation 29. In fitting the data in Figure 18, adjusting E_{5c} and E_{5e} had a strong effect on the decomposition time (the time to C_{out}/C_{in} =0.5), while k_{2br} effected the sharpness of the concentration-time curve. The value k_{2br} affects the reverse of Step 2 and so acts as a bleed on the concentration of the radical species, slowing their initial increase and also speeding their

dissipation at the end of the NCl_3 decomposition reaction. In acting in this way, Step 2br is likely also representing other reactions that could deplete radicals.

In running the model using the constants in Table 3, it was found that the concentration of Cl* rapidly approached its steady-state value. Therefore, to ease calculations, a pseudo-steady state assumption was used for calculating [Cl*]. The concentration of NCl_2* only slowly approached its steady-state value and this effect contributes to the characteristic reaction delay seen in Figures 18 and 19 and also the literature data in Figure 9.

A key issue is that the model predicts a decrease in reaction rate with increasing pressure over the pressures used in this testing which was not seen in the data (see Figure 19). Such a prediction is consistent with the literature on NCl_3 decomposition (see, for example, Figure 9), and in the model it arises from the fitting to the literature data shown in Figure 23. Thus, a potential contribution to this discrepancy is the possibility of non-random experimental errors. The test system was designed for temperature control with around +/- 5°C error, based on an initial plan for experiments at every 10°C and the assumption that at the higher pressures used in this work the reactions would behave more like the apparent first order rate reported for the NCl_3 decomposition in liquid chlorine. However, on testing it was found that the reaction went from little reaction at 55°C to almost complete reaction at 65°C (as shown in Figure 17), indicating an extreme temperature sensitivity for the NCl_3 decomposition reaction. This means the test results are likely sensitive to factors that could affect the temperature control of the gases in the decomposition reactor. Some of these factors include the lab ambient temperature, heat transfer from the gases to the tubing walls, and the heat capacity of the gas flow. Carrying out tests at different pressures, but with the same retention time in the decomposition reactor involves changes to gas flows and gas densities which can result in a non-random drift in the true gas temperature in the decomposition reactor. For example, a higher mass flow of gas at higher pressures would result in a lower temperature loss as the gas flows from the oil bath gas pre-heater to the entrance of the decomposition reactor. This could lead to less under-estimation of the reaction rate at higher pressures.

Data at a wider range of temperatures would be helpful in improving the model. However, because of the very rapid change in the rate of the overall decomposition reaction with temperature, such work would require a wide range of decomposition reactor sizes. The model also does not include the gas heating effects from the reaction enthalpy. This would become more important as the concentration of NCl_3 increases and would be expected to become a dominant factor in the reaction acceleration at NCl_3 concentrations approaching ~3 mole% above which Baillou reported deflagrations can occur (28).

Finally, the model could easily be adjusted to include the effect of the Monel knitted wire mesh pads. The approach used was based on the literature observation that nickel wire could be used to remove Cl*, but with no detectable heterogeneous reaction of NCl_2* (26). It was found that simply by including a Step for first order Cl* surface quenching, the Monel results could be approximately fitted without having to make any other changes to the model.

10.3 A vaporiser concept for contaminated liquid chlorine

The gas-phase NCl_3 destruction demonstrated in this work could be used following a plug-flow vaporiser as described by Brereton and Berretta (23). An alternative approach to safely vaporising NCl_3 contaminated liquid chlorine could also be carried out using an NCl_3-free stream of warm chlorine gas to evaporate liquid chlorine. By using an NCl_3-free stream of chlorine gas

with a controlled temperature, the relative evaporation rates of NCl_3 and chlorine from a liquid feed could be controlled to limit the build-up of NCl_3 in the liquid pool. This is because the dilution effect of the NCl_3-free chlorine gas helps enhance the relative vaporisation of NCl_3 from the liquid chlorine. The concept is shown in Figure 24. The resulting NCl_3 containing chlorine gas is recycled to the decomposition step to re-generate fresh NCl_3-free chlorine. Excess gas from the vaporised liquid will exit the recycle loop. Such a vaporiser could operate at close to atmospheric pressure and so around -34°C.

Based on the heat of vaporisation of liquid chlorine and the heat capacity of chlorine gas, for gas heated to 85°C it will take ~5 moles of chlorine gas to provide enough heat to vaporise 1 mole of liquid chlorine. This will effectively dilute the NCl_3 in the exit gas phase and, roughly proportionally, dilute the equilibrium concentration of NCl_3 that exists in the evaporating liquid. Using an estimated activity coefficient (using l_{12} = 0.112), one can estimate the steady-state concentration of NCl_3 in the evaporating liquid pool in equilibrium with the exiting gas. For a feed of 100 ppm NCl_3, for a simple pooling boiling vaporiser at -34°C with no decomposition, the steady-state exit gas concentration would be 100 ppm and the equilibrium concentration of NCl_3 in the boiling liquid be ~900 ppm (see Figure 4). If 5 moles of 85°C, NCl_3-free chlorine gas are used to evaporate 1 mole of the liquid chlorine, the steady-state exit gas concentration would be ~17 ppm and the equilibrium concentration of NCl_3 in the evaporating liquid be ~150 ppm. Thus, this approach could be used to evaporate liquid chlorine a close to ambient pressure with minimal concentrating of NCl_3 in the liquid chlorine.

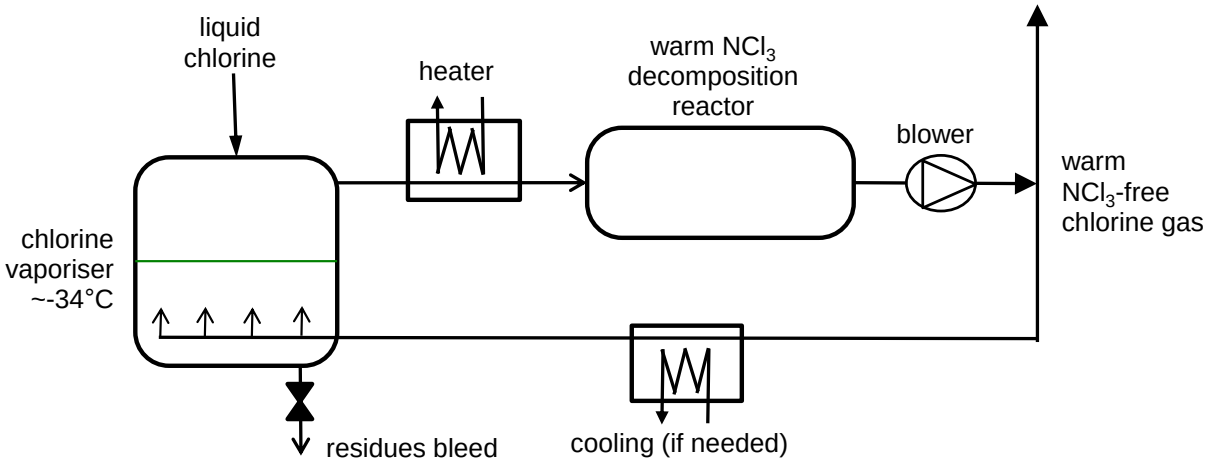

Figure 24: Concept for an atmospheric pressure liquid chlorine vaporizer designed to avoid NCl_3 build-up in the evaporating chlorine pool.

11. Conclusions

The decomposition reaction of NCl_3 was found to be very temperature sensitive. This temperature sensitivity is likely related to the auto-accelerating nature of the decomposition reaction. While the reaction was very sensitive to temperature, it was not sufficiently unstable at close to ambient conditions for the use of a local hot spot to be able to initiate a self-propagating reaction that could then continue after the gas moved away from the hot location.

The influence of pressure on the reaction rate is not clear. The experimental data shows no clear effect over a range from 1.36 to 3.42 bara measured at ~60°C. However, both the literature and the developed model would predict a decrease in rate. It is possible that limitations of the experimental equipment might allow the gas temperature at the entrance of the decomposition reactor to increase slightly with increased pressure (increased gas density and heat capacity), thus offsetting the effect of pressure on the reaction rate. Therefore, the effect of pressure requires further work to be properly clarified. In any future work, the test system design must also provide for very precise and accurate control of the gas temperature.

A simple model has been developed that can approximately fit the experimental data found in this work. The mechanism steps and many of the reaction rate constants used in the model are also consistent with previous literature.

This work has shown that with sufficient temperature and retention time, gaseous NCl_3-contaminated chlorine can be treated to remove NCl_3. The temperatures required are not severe, ambient or close to ambient pressures can be used, and the required retention times are not unreasonable.

12. References

1. "Maximum Levels of nitrogen trichloride in liquid chlorine", GEST 76/55 10th Edition, Euro Chlor Publication, (2001).
2. "Pamphlet 152: Safe Handling of Chlorine Containing Nitrogen Trichloride, Ed. 3", The Chlorine Institute, Inc., Washington, D.C., www.Cl2.com, July (2011).
3. Weil and J.C. Morris, "Kinetic Studies on the Chloramines. I. The Rates of Formation of Monochloramine, N-Chlormethylamine and N-Chlordimethylamine", JACS, 71 (1949) 1664-71.
4. W.A. Noyes and W.F. Tuley, "Heat of Formation of Nitrogen Trichloride", J. Am. Chem. Soc., 47 (1925) 1336-41.
5. W.L Jolly, "The Thermodynamic Properties of Chloramine, Dichloramine and Nitrogen Trichloride", J. Phys. Chem., 60 (1956) 507-8.
6. M. Kothe and W. Hasenpusch, "The formation of explosive chlorine-nitrogen compounds during the processes of precious metals separation", J. Hazard. Mat., 56 (1997) 137-48.
7. H Piersma, "Nitrogen Trichloride: a Continuing Challenge", TSEM 01/274, Euro Chlor Technical Seminar Report (2001).
8. Ya Apin, "Uber einige Sprengeigenschaften von Stickstoffchlorid" (Concerning Explosive properties of Nitrogen Trichloride), Acta Physiochim. URSS, 13 (1940) 405.
9. B.E. Poling, J.M. Prausnitz and J.P. O'Connell, "The Properties of Gases and Liquids, 5th Ed.", McGraw Hill, (2001).
10. C.L. Yaws, "Yaws Handbook of Antoine Coefficients for Vapor Pressure, 2nd Electronic Edition", Knovel, (2009).
11. R.L Zeller III and J.P. DeJac, "Non-ideal solution behavior of NCl_3 in liquid chlorine and its implications", Pamphlet 21 - Edition 6, The Chlorine Institute, Inc., Washington, D.C., www.CL2.com, (2010) 216-40.
12. "Reproduction of Chlorine Institute reports concerning NCl_3", in "Nitrogen trichloride – A collection of reports and papers", Pamphlet 21 - Edition 6, The Chlorine Institute, Inc., Washington, D.C., www.CL2.com, (2010) 21-41.
13. R.E. Ross and J.L. Bowling "NCl_3 Concentrations and decomposition by dry compression" (1963) in "Pamphlet 21: Nitrogen Trichloride – A Collection of Reports and Papers, Edition 6", The Chlorine Institute, Inc., (2010) p. 84-89.

14. M. Knothe and W. Hasenpusch, “Formation of explosive chlorine-nitrogen compounds during the reaction of ammonium compounds with chlorine”, Inorg. Chem., 35 (1996) 4529-30.
15. B.S. Yiin and D.W. Margerum, “Non-Metal Redox Kinetics: Reactions of Trichloramine with Ammonia and with Dichloramine”, Inorg. Chem., 29 (1990) 2135-2141.
16. A. Heilborn, “On Nitrogen Trichloride Hazards” (1962) in “Pamphlet 21: Nitrogen Trichloride – A Collection of Reports and Papers, Edition 6”, The Chlorine Institute, Inc., (2010) p. 47-50.
17. T.F. O’Brien, T.V. Bommaraju and F. Hine, “Handbook of Chlor Alkali Technology”, Springer Science, Vol. 3 Ch. 9 (2005) 765-1011.
18. J.L. Gustin, “Safety of chlorine production and chlorination processes”, Chem Health & Safety, 5-16.
19. V.A. Shushunov and L.Z. Pavlova, “Decomposition of Nitrogen Trichloride in a Carbon Tetrachloride Solution”, Journal of Inorganic Chemistry (USSR), 2(9) (1957) 446-8. (Zhurn. Neorg. Khim. 2 (1957) 2272-4.)
20. “Use of CTC in the elimination of NCl_3 in the production of chlorine and caustic soda”, Process Agents Task Force, Montreal Protocol, UNEP, May 2001, www.teap.org
21. C.T. Jafvert and R.L. Valentine, “Reaction Scheme for the Chlorination of Ammoniacal Water”, Environ. Sci. Technol., 26(3) (1992) 577-86.
22. K. Kumar, R.W. Shinness and D.W. Margerum, “Kinetics and Mechanisms of the Base Decomposition of Nitrogen Trichloride in Aqueous Solution”, Inorg. Chem., 26 (1987) 3430-4.
23. C. Brereton and S. Berretta, “Method and Apparatus for Vaporizing Liquid Chlorine Containing Nitrogen Trichloride”, US 2012/0017848 A1, Jan. 26, 2012.
24. V.V. Azatyan, R.R. Borodulin, E.A. Markevich, N.M. Rubtsov and N.N. Semenov, “Isothermal Propagation of Rarefied Nitrogen Trichloride Flames”, Bulletin of the Academy of Sciences of the USSR, Division of chemical science, 25(7) (1976) 1396-7 (Izvestiya Akademii Nauk SSSR Seriya Kimicheskaya 7 (1976) 1459-61).
25. J.G.A. Griffiths and R.G.W. Norrish, “The Photosensitised Decomposition of Nitrogen Trichloride Part 1”, Proc. Roy. Soc. Lond. A, 130 (1931) 591-609.
26. T.C. Clark and M.A.A. Clyne, “Kinetic Mechanisms in Nitrogen-Chlorine Radical Systems, Part 1”, Trans. Faraday Soc., 65 (1969) 2994-3004.
27. P.G. Ashmore, “Explosions in mixtures of hydrogen, chlorine and nitrogen trichloride”, Nature 172 (1953) 449-50.
28. F. Baillou, “Proprietes explosives du trichlorure d'azote gazeux” (Explosive properties of gaseous nitrogen trichloride), Ph.D. Thesis, U. Orleans, (1990).
29. J.G.A. Griffiths and R.G.W. Norrish, “The Photosensitised Decomposition of Nitrogen Trichloride and the Induction Period of the Hydrogen-Chlorine Reaction”, Trans. Faraday Soc., 27 (1931) 451-458.
30. J.G.A. Griffiths and R.G.W. Norrish, “The Photosensitised Decomposition of Nitrogen Trichloride Part 2: The Effects of Surface and Inert Gases and the Mechanism of Reaction”, Proc. Roy. Soc. Lond. A, 135 (1932) 69-83.
31. T.C. Clark and M.A.A. Clyne, “Free Radicals formed in the Induced Decomposition of Nitrogen Trichloride”, Symp (Int.) on Combustion, 12 (1969) 333-343.
32. T.C. Clark and M.A.A. Clyne, “Kinetic Mechanisms in Nitrogen-Chlorine Radical Systems, Part 2”, Trans. Faraday Soc., 66 (1970) 372-385.
33. W.B. Demore, S.P. Sander, D.M. Golden, R.F. Hampson, M.J. Kurylo, C.J. Howard, A.R. Ravishankara, C.E. Kolb and M.J. Molina, “Chemical kinetics and photochemical data for use in stratospheric modeling, Evaluation No. 12” JPL Publication 97-4 (1997).
34. V.V. Azatyan, R.R. Borodulin and E.A. Markevich, “Identification of chlorine atoms in a low-density nitrogen trichloride flame”, Kinetics and Catalysis, 15 (1974) 1427-8. (Kinetika i Kataliz, 15 (1974) 1610.)

35. R.R. Borodulin, E.A. Markevich, V.V. Azatyan and N.N. Semenov, “Determination of the atomic chlorine concentration in a low-density nitrogen trichloride flame”, Kinetics and Catalysis, 17 (1976) 730-2. (Kinetika i Kataliz, 17 (1976) 834-6.)
36. V.V. Azatyan, R.R. Borodulin, E.A. Markevich and N.M. Rubtsov, “Kinetics of NCl_3 decomposition in an attenuated flame”, Combustion, Explosion, and Shock Waves, 14(2) (1978) 146-50. (Fizika Goreniya i Vzryva, 14(2) (1978) 20-6).
37. N.M. Rubtsov and V.D. Kotelkin, “Transition from isothermal to chain-thermal flame-propagation regimes in the branching-chain decomposition of nitrogen trichloride”, Mendeleev Commun., 12(1) (2002) 33–35.
38. V. V. Azatyan, R. R. Borodulin and N. M. Rubtsov, “Nonthermal Propagation of the Flame of Nitrogen Trichloride”, Combustion, Explosion, and Shock Waves, 15(5) (1979) 583-8. (Fizika Goreniya i Vzryva, 15(5) (1979) 34-40).
39. H.H. Sisler, F.T. Neth, R.S. Drago and D. Yaney, “The Synthesis of Chloramine by the Ammonia-Chlorine Reaction in the Gas Phase”, J. Am. Chem. Soc., 76 (1954) 3906-9.
40. Working party of the bureau international technique du chlore, “The determination of nitrogen trichloride in liquid chlorine”, Analytica Chimica Acta, 156 (1984) 221-33.
41. F.H. Walters, K.B. Griffin and D.F. Keeley, “Use of Ammonia-sensing Electrodes in Salt Media”, Analyst, 109 (1984) 663-5.
42. “User Guide - High Performance Ammonia Ion Selective Electrode”, Thermo Fisher Scientific Inc., (2007).
43. G.P. Kota, J.W. Coburn and D.B. Graves, “The recombination of chlorine atoms at surfaces”, J. Vac. Sci. Technol. A, 16(1) (1998) 270-7.
44. P.G. Ashmore, A.J. Parker and D.E. Stearne, “Recombination of Chlorine Atoms on Surfaces”, Trans. Faraday Soc., 67 (1971) 3081-93.
45. A. Farmer, “Laboratory and Developmental Work on Ultraviolet Light for Removal of Nitrogen Trichloride from Chlorine Gas”, Pamphlet 21 - Edition 6, The Chlorine Institute, Inc., Washington, D.C., www.CL2.com, (2010) 51-8.
46. M.A.A. Clyne and D.H. Stedman, “Recombination of Ground-State Halogen Atoms, Part 1”, Trans. Faraday Soc., 64 (1968) 1816-35.
47. M.A.A. Clyne and D.H. Stedman, “Recombination of Ground-State Halogen Atoms, Part 2”, Trans. Faraday Soc., 64 (1968) 2698-2707.
48. G. Huybrechts, Y. Hubin, B. Van Mele, “Kinetics and Mechanism of the Thermal Chlorination of Chloroform in the Gas Phase”, Int. J. Chem. Kin., 32 (2000) 466-71.
49. B.D. Darwent, “Bond dissociation energies in simple molecules”, Nat. Std. Data Ref. Ser., Nat. Bur. Stand., NSDRS-NBS 31 (1970).
50. M.A.A. Clyne and D.H. Stedman, “Recombination of Ground State Halogen Atoms Part 2. Kinetics of the Overall Recombination of Chlorine Atoms”, Trans. Faraday Soc., 64 (1968) 2698-707.
51. H.H. Carstensen and A.M. Dean, “The Kinetics of Pressure-Dependent Reactions” in “Comprehensive Chemical Kinetics”, Vol. 42 (2007) 105-87.
52. N.M. Rubtsov, “Kinetic mechanism and chemical oscillations in the branching-chain decomposition of nitrogen trichloride”, Mendeleev Commun., 5 (1998) 173-5.
53. N. M. Rubtsov and V. D. Kotelkin, “Propagation of Isothermal Flame in the Low-Pressure Thermal Decomposition of Nitrogen Trichloride”, Theor. Found. Chem. Eng., 36(4) (2002) 370–381 (Teoreticheskie Osnovy Khimicheskoi Tekhnologii, 36(4) (2002) 405–417.
54. W.B. DeMore, S.P. Sander, D.M. Golden, R.F. Hampson, M.J. Kurylo, C.J. Howard, A.R. Ravishankara, C.E. Kolb and M.J. Molina, “Chemical Kinetics and Photochemical Data for Use in Stratospheric Modeling, Evaluation Number 10”, JPL Publication 92, NASA-CR-192795 (1992).